

See discussions, stats, and author profiles for this publication at: <https://www.researchgate.net/publication/243835805>

Stereochemical Models for Discussing Additions to α , β Unsaturated Aldehydes Organocatalyzed by Diarylprolinol or Imidazolidinone Derivatives – Is There an ‘(E)/(Z)Dilemma’ ?

ARTICLE in *HELVETICA CHIMICA ACTA* · APRIL 2010

Impact Factor: 1.14 · DOI: 10.1002/hlca.201000069

CITATIONS

45

READS

18

8 AUTHORS, INCLUDING:



Uroš Grošelj

University of Ljubljana

118 PUBLICATIONS 1,062 CITATIONS

SEE PROFILE



Gildas Deniau

Polyphor AG

16 PUBLICATIONS 208 CITATIONS

SEE PROFILE



Christof Sparr

University of Basel

29 PUBLICATIONS 468 CITATIONS

SEE PROFILE

Stereochemical Models for Discussing Additions to α,β -Unsaturated Aldehydes Organocatalyzed by Diarylprolinol or Imidazolidinone Derivatives – Is There an '(E)/(Z)-Dilemma'?

by **Dieter Seebach***, **Ryan Gilmour*¹⁾**, **Uroš Grošelj²⁾**, **Gildas Deniau³⁾**, **Christof Sparr⁴⁾**,
Marc-Olivier Ebert*, and **Albert K. Beck**

Laboratorium für Organische Chemie, Departement für Chemie und Angewandte Biowissenschaften,
ETH Zürich, Hönggerberg, Wolfgang-Pauli-Strasse 10, CH-8093 Zürich
(phone: +41-44-632-2990; fax: +41-44-632-1144; e-mail: seebach@org.chem.ethz.ch; phone: +41-44-
632-7934; fax: +41-44-633-1235; e-mail: ryan.gilmour@org.chem.ethz.ch; phone: +41-44-633-4726;
e-mail: marc-olivier.ebert@org.chem.ethz.ch)

and **Lynne B. McCusker** and **Dubravka Šišak⁵⁾**

Laboratorium für Kristallographie, Departement Materialwissenschaft, ETH Zürich, Hönggerberg,
Wolfgang-Pauli-Strasse 10, CH-8093 Zürich (phone: +41-44-632-3721;
e-mail: lynne.mccusker@mat.ethz.ch)

and **Tadafumi Uchimaru**

Research Institute for Computational Sciences, National Institute of Advanced Industrial Science and
Technology (AIST), Tsukuba, Ibaraki 305-8568, Japan (phone: +81-29-861-4800;
e-mail: t-uchimaru@aist.go.jp)

Dedicated to Professor *Henri Kagan* on the occasion of his 80th birthday

The structures of iminium salts formed from diarylprolinol or imidazolidinone derivatives and α,β -unsaturated aldehydes have been studied by X-ray powder diffraction (*Fig. 1*), single-crystal X-ray analyses (*Table 1*), NMR spectroscopy (*Tables 2* and *3*, *Figs. 2–7*), and DFT calculations (*Helv. Chim. Acta* **2009**, *92*, 1, 1225, **2010**, *93*, 1; *Angew. Chem., Int. Ed.* **2009**, *48*, 3065). Almost all iminium salts of this type exist in solution as diastereoisomeric mixtures with (*E*)- and (*Z*)-configured $^+N=C$ bond geometries. In this study, (*E*)/(*Z*) ratios ranging from 88:12 up to 98:2 (*Tables 2* and *3*) and (*E*)/(*Z*) interconversions (*Figs. 2–7*) were observed. Furthermore, the relative rates, at which the (*E*)- and (*Z*)-isomers are formed from ammonium salts and α,β -unsaturated aldehydes, were found to differ from the (*E*)/(*Z*) equilibrium ratio in at least two cases (*Figs. 4* and *5, a*, and *Fig. 6, a*); more (*Z*)-isomer is formed kinetically than corresponding to its equilibrium fraction. Given that the enantiomeric product ratios observed in reactions mediated by organocatalysts of this type are often $\geq 99:1$, the (*E*)-iminium-ion

¹⁾ *Alfred Werner* Assistant Professor of Synthetic Organic Chemistry at the ETH Zürich.

²⁾ On leave from Faculty of Chemistry and Chemical Technology, University of Ljubljana, Aškerčeva 5, P.O. Box 537, 1000 Ljubljana, Slovenia; financed by *Slovene Human Resources Development and Scholarship Fund* (Vilharjeva 27, 1000 Ljubljana, Slovenia) and by *Novartis Pharma AG*, Basel.

³⁾ Postdoctoral Fellow, ETH Zürich (2007–2009), financially supported by the *Swiss National Science Foundation* (Project No. 200020-117586) and by *Novartis Pharma AG*, Basel.

⁴⁾ Part of the projected Ph.D. thesis of C. S. ETH Zürich; financially supported by the *Roche Research Foundation*, Basel, and a *Novartis Doctoral Fellowship*.

⁵⁾ Ph.D. Student financially supported by the *Swiss National Science Foundation* (Project No. 200020-117677).

intermediates are proposed to react with nucleophiles faster than the (*Z*)-isomers (*Scheme 5* and *Fig. 8*). Possible reasons for the higher reactivity of (*E*)-iminium ions (*Figs. 8* and *9*) and for the kinetic preference of (*Z*)-iminium-ion formation are discussed (*Scheme 4*). The results of related density functional theory (DFT) calculations are also reported (*Figs. 10–13* and *Table 4*).

1. Introduction. – Since the renaissance of organocatalysis⁶⁾ in 2000 [3], this field has undergone an explosive development⁷⁾. Of the various types of organocatalysts, compounds with a *sec*-amino group (proline and its derivatives, including diarylprolinol ethers [5], and amino acid (mostly phenylalanine)-derived imidazolidinones [3b]) have experienced the widest use. They activate α -carbonyl positions for electrophilic attack⁸⁾ through enamines and β -carbonyl positions for nucleophilic attack through iminium ions, thus opening the door to enantioselectively catalyzed versions of the most important classical synthetic organic reactions⁹⁾. Entire sequences of such reactions can be performed with one organocatalyst, or with two different species, culminating in the formation of four and more stereogenic centers *via* so-called domino or cascade reactions [8]. However, much of the mechanistic intricacies of organocatalytic transformations remain unexplored; a casualty of the excitement that the synthetic competence of this class of small molecules has generated. Often reasonable mechanistic models are proposed that are based solely on the stereochemical outcome of the transformation in question.

On closer inspection, aspects of many commonly accepted mechanistic models were identified that led to the proposal of possible alternatives. Thus, in proline catalysis, the role of oxazolidinones may not just be part of a parasitic [9] equilibrium (*Eqn. 1*) [10]. Moreover, structural and theoretical investigations of reactive intermediates in catalyses with diarylprolinol ethers have revealed that the facial selectivity, with which the derived enamines and iminium ions react, is probably not caused by a benzene ring but by the ether RO group and a *meta*-substituent *on* the benzene ring [11][12], while it is likely that the benzene ring provides shielding in the corresponding fluoro derivative [13] (see *Eqn. 2*). Finally, the more electrophilic iminium ions derived from 5-benzyl-imidazolidinones¹⁰⁾ appear to exist as an equilibrating mixture of conformers around the exocyclic benzylic ethane bond, in which the conformer with the Ph group over the heterocyclic ring (and not, as commonly assumed, over the π -system) generally prevails (according to DFT, NMR, and X-ray investigations) (*Eqn. 3*) [11][15][16]. Here, we

⁶⁾ The term ‘organic catalyst’ (‘organischer Katalysator’) has been used by the school of *Langenbeck* and is the title of a book, which appeared in 1935 [1]; an observation of *J. v. Liebig*’s concerning an organocatalytic reaction (see footnote on page 14/15 in [2]) is discussed therein.

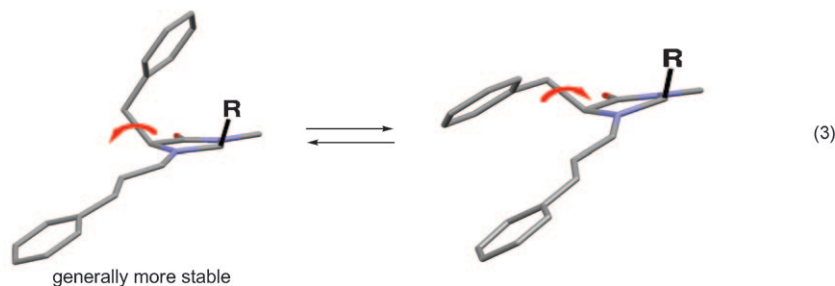
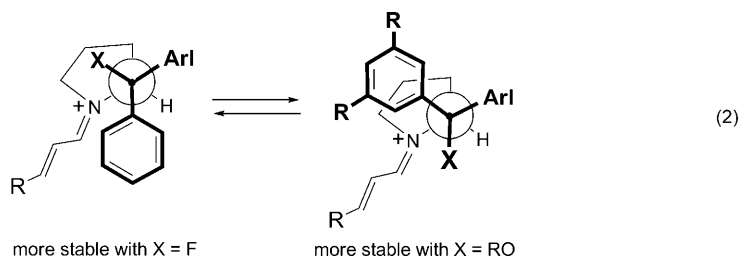
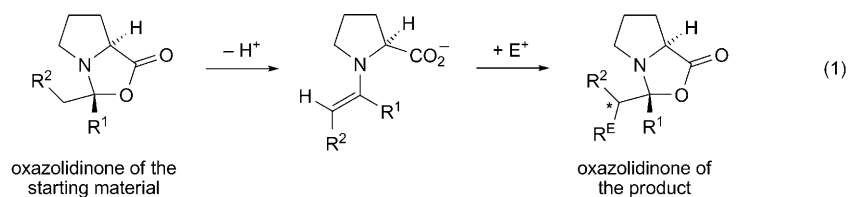
⁷⁾ For recent review articles, in which the historic background is discussed, see [4] (‘Organocatalysis Lost: Modern Chemistry, Ancient Chemistry, and an Unseen Biosynthetic Apparatus’ [4a]; ‘The advent and development of organocatalysis’, ‘History and Perspectives of Chiral Organic Catalysts’ [4b]; ‘Emil Knoevenagel and the Roots of Aminocatalysis’ [4c]).

⁸⁾ Radical reactions in α -carbonyl position can also be achieved enantioselectively with the help of organocatalysts (*cf.* oxidation of an intermediate enamine with Fe^{III} or Ce^{IV} complexes to cation radicals, ‘SOMO activation’ [6]).

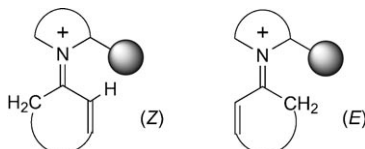
⁹⁾ The chemistry of carbonyl compounds has been called ‘the backbone of organic synthesis’ [7].

¹⁰⁾ The cinnamaldehyde derivative of 5-benzyl-2,3,3-trimethylimidazolidinone is by one order of magnitude more reactive than that of diphenylprolinol trimethylsilyl ether [14].

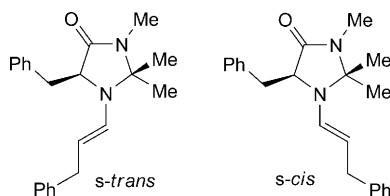
present results, which reveal new aspects about another supposition, according to which only (*E*)-iminium ions are present (*Eqn. 4*), when an α,β -unsaturated aldehyde is activated upon reaction with a diarylprolinol or an imidazolidinone derivative¹¹⁾¹²⁾.

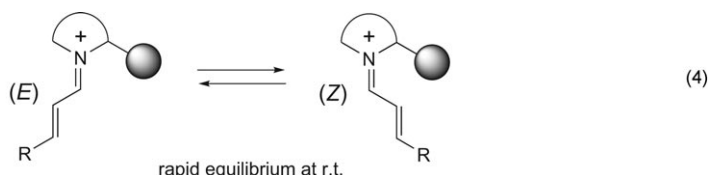


¹¹⁾ With α,β -unsaturated ketones, the energy difference between the (*E*)- and (*Z*)-forms may be small and may lead to the reversal of the stereochemical course of reactions, as compared to those of α,β -unsaturated aldehydes [17].



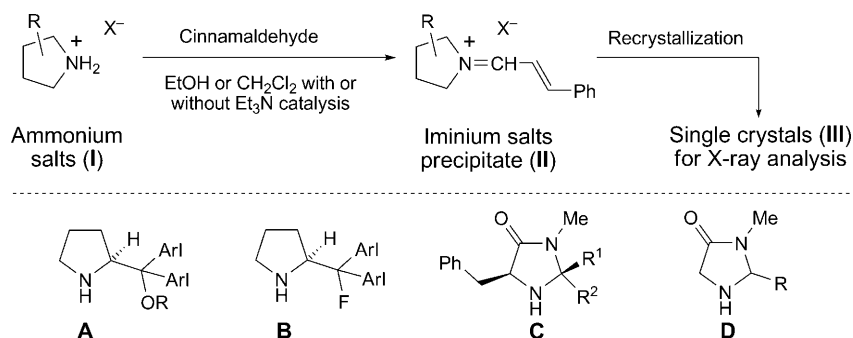
¹²⁾ Yet another isomerism was discovered by Gellman and co-workers (see [18]): there are NMR-detectable amounts of the *s-cis*-conformer of the enamine formed from hydrocinnamaldehyde and benzyl-trimethyl-imidazolidinone.





2. (E)/(Z)-Isomeric Iminium Salts E, F, and G in the Solid State: X-Ray Crystal Structures. – To initiate a systematic solid-state study the iminium ion salts derived from cinnamaldehyde and diaryl-prolinol derivatives, **A** and **B**, or imidazolidinones, **C** and **D**, were prepared by modifying the procedure of *Leonard and Paukstelis* [19], in which an ammonium salt, **I**, of a *sec*-amine is mixed with a carbonyl compound in EtOH or CH₂Cl₂ (with or without Et₃N catalysis). This yielded a precipitate or residue, which was washed and dried to give the iminium salts of correct elemental analyses (*cf.* **II** in *Scheme 1*). From solutions of these precipitated salts single crystals, **III**, were grown as described in earlier reports [11–16][20]. The compounds, of which X-ray crystal structures have been obtained, are listed in *Table 1*. As can be seen from this table, the majority of the structures of the type **E** (diarylprolinol derivatives) and **F/G** (imidazolidinone derivatives) have (*E*)-configured ⁺N=C bonds.

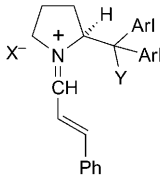
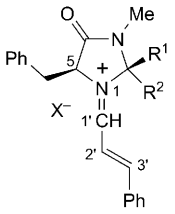
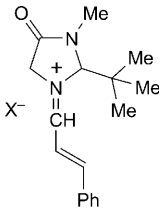
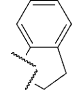
Scheme 1. Preparation of Iminium Salts from Ammonium Salts of the Amino Compounds **A**, **B**, **C**, or **D**, and Cinnamaldehyde



The configuration of the molecules in the single crystals¹³), **III**, need not, of course, be the same as in the original precipitate, **II**: the single crystals are grown very slowly, while the precipitate is formed rapidly. To compare the structures in the precipitated solids with those in the carefully grown crystals, we have determined X-ray powder-diffraction patterns of some non-recrystallized materials (*i.e.*, **II**). These patterns arise from the very small crystallites in the ‘powder’ [21] and can even be used to determine the structures of organic compounds in certain cases, if single crystals are unattainable [22]. Conversely, the X-ray powder-diffraction pattern can be produced easily with a ‘mouse click’, given the atomic coordinates of a crystal structure. In this particular case,

¹³) Full experimental details and characterizations of all compounds mentioned herein have either been published previously [12][13] or will be the subject of a forthcoming full paper in this journal.

Table 1. Configuration of Cinnamoylidene-iminium Salts **E**, **F**, and **G** in Single-Crystal X-Ray Structures

<div style="display: flex; justify-content: space-around; align-items: center;"> <div style="text-align: center;">  <p>E</p> </div> <div style="text-align: center;">  <p>F</p> </div> <div style="text-align: center;">  <p>G</p> </div> </div>				
E	Arl	Y	X	Configuration of the N=C Bond
	Ph	F	ClO ₄	(<i>Z</i>)
	Ph	Me ₃ SiO	BF ₄	(<i>E</i>)
	Ph	(Me)(Ph) ₂ SiO	BF ₄	(<i>E</i>)
	3,5-Me ₂ -C ₆ H ₃	MeO	BF ₄	(<i>E</i>)
	3,5-Me ₂ -C ₆ H ₃	MeO	PF ₆	(<i>E</i>)
	3,5-(CF ₃) ₂ -C ₆ H ₃	MeO	Al[OC(CF ₃) ₃] ₄	(<i>E</i>)
	3,5-(CF ₃) ₂ -C ₆ H ₃	Me ₃ SiO	Al[OC(CF ₃) ₃] ₄	(<i>E</i>)
F	R ¹	R ²	X	Configuration of the N=C Bond
	Et	H	PF ₆	(<i>E</i>)
	<i>i</i> Pr	H	PF ₆	(<i>E</i>)
	<i>t</i> Bu	H	PF ₆	(<i>E</i>)
	Ph	H	PF ₆	(<i>E</i>)
	(<i>E</i>)-Et-CH=C(Me)	H	PF ₆	(<i>E</i>)
	(<i>E</i>)-Ph-CH=CH	H	PF ₆	(<i>E</i>)
	Me	Me	BF ₄ , ClO ₄ , PF ₆	(<i>E</i>)
	Me	FCH ₂	PF ₆	(<i>E</i>)
	<i>i</i> Pr	Me	PF ₆	(<i>E</i>)
	<i>t</i> Bu	Me	PF ₆	(<i>E</i>)
	Ph	Me	PF ₆	(<i>Z</i>)
	spiro 		PF ₆	(<i>Z</i>)
G			BF ₄	(<i>E</i>)

the experimentally determined and calculated profiles of a diarylprolinol-derived and of three imidazolidinone-derived iminium salts were compared using the *Rietveld* refinement program XRS-82 [23] (*Fig. 1*). It is interesting to note that the ‘spectra-like’ patterns are essentially identical in these four cases: unequivocal evidence to establish that species in the crystalline domains of the original precipitates (**II** in *Scheme 1*) and in the single crystals are identical. A potential pitfall of this analysis could be that the precipitate consists of a mixture of microcrystalline material (generating the pattern) and of totally amorphous material (contributing only to the background of the pattern), in which the molecules may adopt another structure. Of the four patterns shown in *Fig. 1*, for example, the bottom two have a somewhat higher background contribution than the others. To ensure that the precipitate and the single crystals comprise the same isomeric iminium salts and are both uniform, we have dissolved

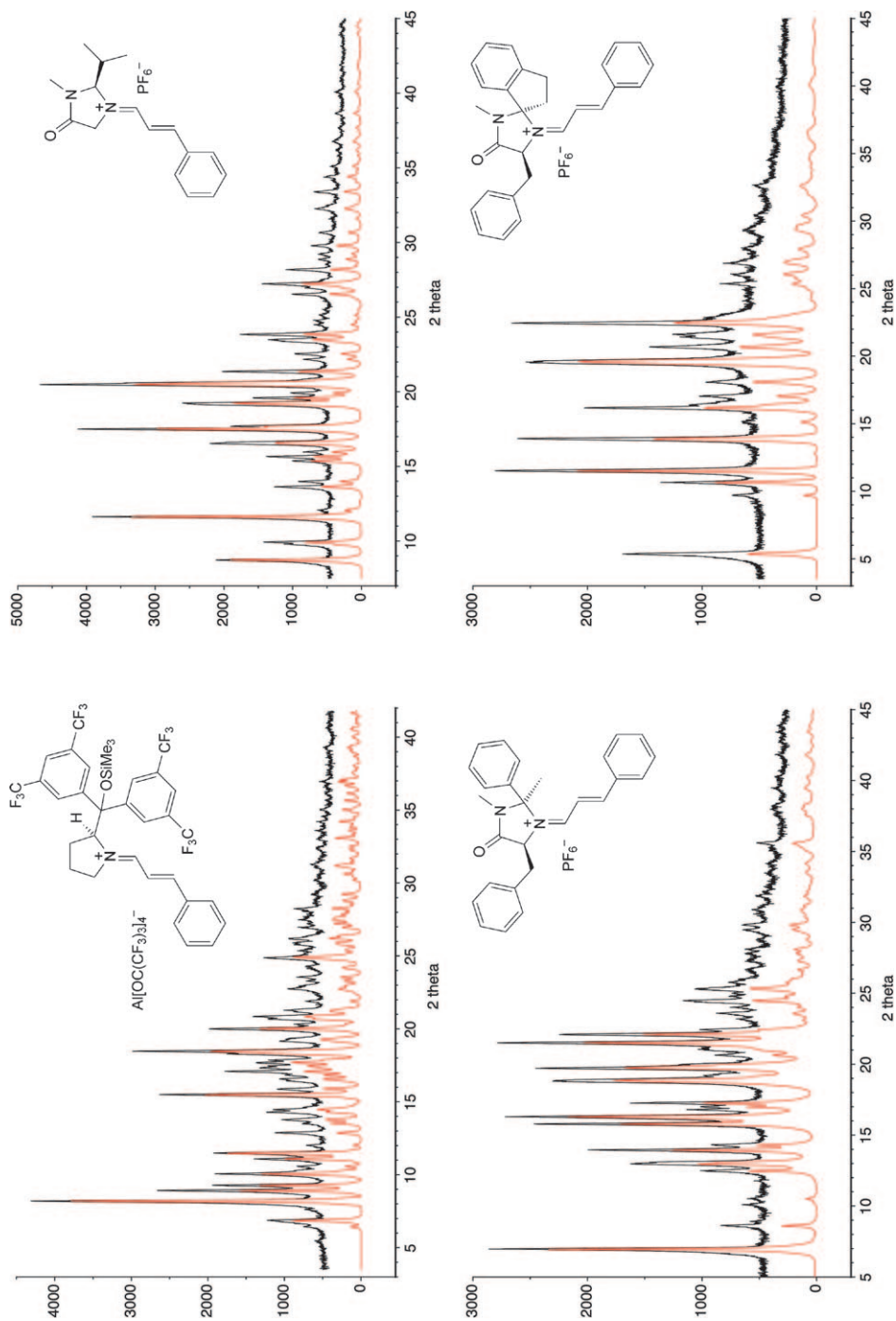
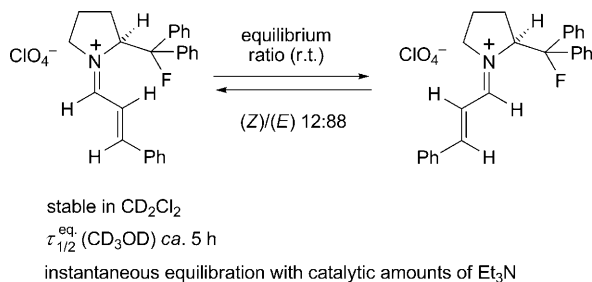


Fig. 1. X-Ray powder diffraction patterns of a diarylprolinol- and of three imidazolidinone-derivedinium salts. The black profiles were recorded with the original salt precipitates (**II** in Scheme 1) and the red ones were calculated from the corresponding single-crystal (**III** in Scheme 1) coordinates.

representative samples in various solvents and at various temperatures, and recorded NMR spectra.

3. The Configurations of Cinnamaldehyde-Derived Iminium Salts of Type E, F, and G in Solution: ¹H-NMR Spectra. – Initially, the fluoro derivative shown in *Scheme 2* was investigated; it has (*Z*)-configuration in single crystals, and the NMR spectrum shows exclusively the (*Z*)-form in CD₂Cl₂. However, when a trace of Et₃N is added, there is instantaneous equilibration with the corresponding (*E*)-isomer. In the ‘protic’ solvent CD₃OD, equilibration¹⁴) occurs with a half-life of *ca.* 5 h. The (*E*)/(*Z*) equilibrium ratio is 88:12 in both solvents. Of the diarylprolinol trimethylsilyl ether-derived iminium salt shown in *Fig. 2* (a reactive intermediate of the *Jørgensen* organocatalyst), we prepared a solution in (D₆)acetone at –50°. Initially, there was only the (*E*)-isomer present within the detection limit of the NMR instrument; upon warming to room temperature, the signals of the (*Z*)-isomer appeared; from the signal integration an (*E*)/(*Z*) equilibrium ratio of 95:5 was derived; the same result was obtained in CD₃CN. Interestingly, a somewhat faster equilibration was observed with the imidazolidinone-derived iminium salt shown in *Fig. 3*; in the single crystals and in the precipitate of this acetophenone derivative (*Table 1* and *Fig. 1*), the molecules have (*Z*)-configuration, and a solution prepared in (D₆)acetone at –30° shows only signals corresponding to the (*Z*)-isomer in the NMR spectrum; warming such a solution to –10° causes equilibration with the (*E*)-isomer leading, at ambient temperature, to an equilibrium ratio (*E*)/(*Z*) of *ca.* 3:1. In *Tables 2* and *3*, the NMR-determined (*E*)/(*Z*) ratios of all diarylprolinol- and imidazolidinone-derived iminium salts, which we have prepared so far, are listed, including those of which we have not been able to determine X-ray crystal structures. Out of the 17 examples, there are only five cases, in which we have not detected both the (*E*)- and the (*Z*)-isomer, independent of counter-ions and only slightly dependent on the solvent. *This includes the derivatives of typical organocatalysts marked in yellow in Tables 2 and 3!*

Scheme 2. The (*Z*)- and (*E*)-Isomers of the Iminium Salt from Cinnamaldehyde and 2-[Fluoro(diphenyl)methyl]pyrrolidine. For details of preparation, see Supplementary Material in [13]. The 1:1 ratio reported in [13] turned out to be the result of an NMR measurement with a solution, which happened to contain the two isomers in this ratio, but in which the equilibrium had not yet been established.



¹⁴) For mechanisms of equilibration, see Scheme 4 in [12].

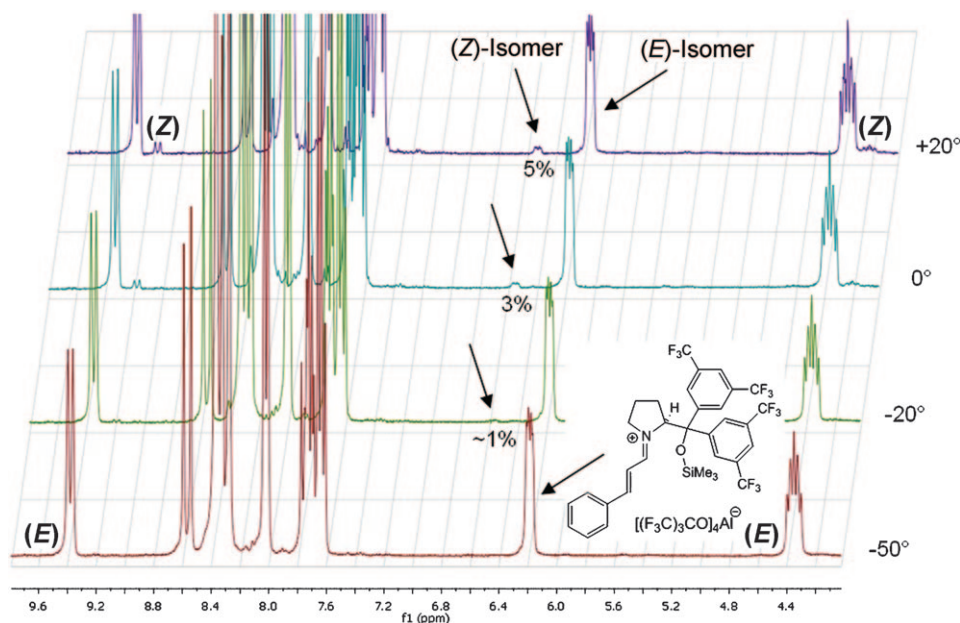


Fig. 2. Temperature-dependent (*E*)/(*Z*)-interconversion of a diarylprolinol-derived iminium salt (type **E**) followed by $^1\text{H-NMR}$. The corresponding precipitate (**II** in Scheme 1) was dissolved in (D_6)acetone at -50° . After recording the spectrum, the sample was allowed to warm to -20° , 0° , and $+20^\circ$; at each temperature it was kept for 1 h before the spectrum was recorded. The same result was obtained in CD_3CN . The equilibrium value given in Table 2 (92:8) was obtained by a different experimentalist; we should be aware of the fact that the equilibration rate may be slow, which can lead to different (*E*)/(*Z*) values, depending upon the period of time between dissolving the sample and actually recording the NMR spectrum (cf. Figs. 2–7).

4. Kinetics of the Formation of Iminium Salts from Imidazolidinones and α,β -Unsaturated Aldehydes. – Following the structural studies, we investigated the actual formation of the iminium salts from various imidazolidinones and cinnamaldehyde, crotonaldehyde or hex-2-enal.

In a preliminary experiment, we first added an equimolar amount of cinnamaldehyde to a CD_3CN solution of the 5-benzyl-2,3-dimethyl-2-phenylimidazolidinium hexafluorophosphate in an NMR tube at -30° and recorded the resulting NMR spectrum at this temperature to see only a broad signal at 8.8 ppm. The NMR probe was then warmed to -20° for 30 min, and a spectrum recorded again, showing *ca.* 7% conversion to iminium ions; intriguingly, the (*Z*)-isomer prevailed ((*E*)/(*Z*) ratio *ca.* 1:3, see Fig. 4, *a*). The NMR tube was then kept in a freezer at -20° for 20 h, and a spectrum was recorded again at this temperature; now the conversion was 15% and the (*E*)/(*Z*) ratio *ca.* 1:2 (Fig. 4, *b*). The (*E*)/(*Z*) equilibrium ratio at room temperature is 4:1 in MeCN and 3:1 in acetone (see Table 3).

In Figs. 5–7, the sections of the $^1\text{H-NMR}$ spectra, where the $^+\text{N}=\text{CH}$ and vinylic $\text{C}=\text{CH}$ signals are expected to be seen at lowest field, are shown for the reactions of three imidazolidinones with the three different aldehydes (molar ratio 1:2), at room

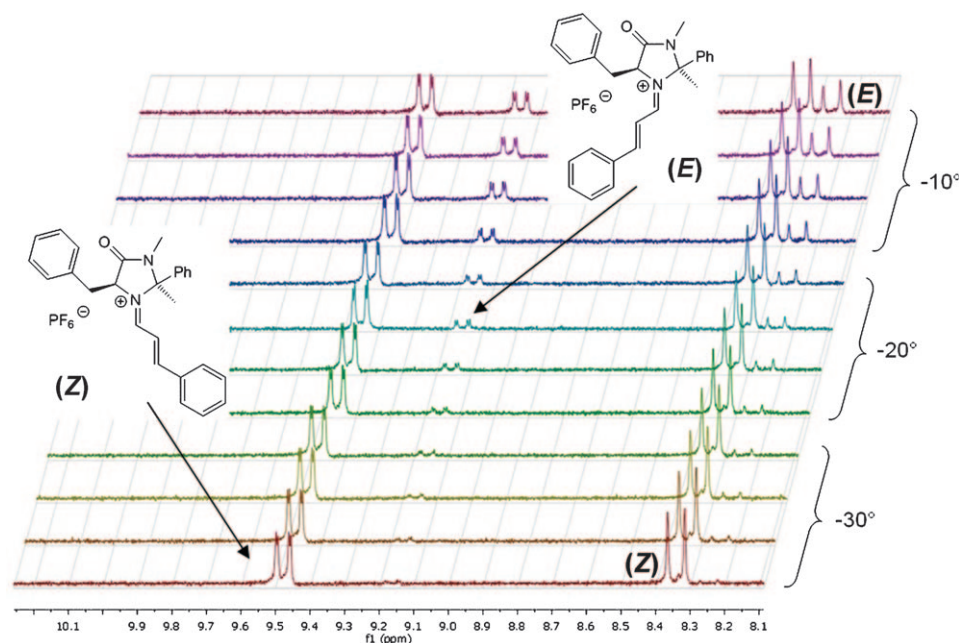


Fig. 3. Temperature-dependent (E)/(Z)-interconversion of an imidazolidinone-derived iminium salt (type **F**) followed by ^1H -NMR. The corresponding recrystallized (**III** in Scheme 1) sample was dissolved in $(\text{D}_6)\text{acetone}$ at -30° . The time between each recording was 3 min, each recording took 4 min; the total time from -30° to -10° was 90 min. A solution prepared at -60° contains $<0.5\%$ (E)-isomer. The equilibrium ratio at room temperature is (E)/(Z) 3:1 (Table 3).

temperature (a total of nine combinations)¹⁵). Safe signal assignments of the (E)- and (Z)-isomers can only be accomplished for the cinnamoylidene derivatives, of which pure samples have been isolated [11][14][15][16]¹³ (see Figs. 5, a, 6, a, and 7, a). For the aliphatic crotonaldehyde (Figs. 5, b, 6, b, and 7, b) and hexenal derivatives (Figs. 5, c, 6, c, and 7, c) assignments are not possible at this stage, and clear-cut NMR monitoring is made difficult by the appearance of signals from side-products (possibly resulting from aldol-type reactions). The general patterns of the spectra suggest, however, that there are geometric isomers also of the iminium salts derived from aliphatic enals in these reaction mixtures, although the occurrence of other types of isomers cannot be totally excluded (see Scheme 3).

In conclusion, incontrovertible evidence has been presented that both types of iminium salts **E** (derived from diarylprolinol) and **F/G** (derived from imidazolidinones), in addition to the corresponding aliphatic derivatives (Me or ^iPr instead of Ph) are mixtures of (E)/(Z)-isomers around the $^+\text{N}=\text{C}$ bond. Before turning to the implication this fact has for organocatalysis, we would like to briefly discuss the kinetic

¹⁵) The % conversions given in Figs. 5 and 6 were determined from the NMR-signal integrations of the H-atoms at C(5) in the ammonium starting materials and iminium products.

Table 2. (*E*)/(*Z*) Ratios of Diarylprolinol-Derived Iminium Salts **E** in Solution (determined by ¹H-NMR analysis at ambient temperatures) [12]

Arl	Y	X	Solvent	(<i>E</i>)/(<i>Z</i>) Ratio
Ph	F	ClO ₄	CD ₂ Cl ₂	88 : 12
	Me ₃ SiO	BF ₄	CDCl ₃	97 : 3
	(Me)(Ph) ₂ SiO	BF ₄	(D ₆)DMSO	97 : 3
4- <i>t</i> Bu-C ₆ H ₄ ^a)	(Me)(Ph) ₂ SiO	BF ₄	CDCl ₃	> 99 : 1
3,5-Me ₂ -C ₆ H ₃	MeO	PF ₆	CDCl ₃	94 : 6
	MeO	BF ₄	CDCl ₃	> 99 : 1
3,5-(CF ₃) ₂ -C ₆ H ₃	MeO	Al[OC(CF ₃) ₃] ₄	(D ₆)DMSO	94 : 6
	Me ₃ SiO	PF ₆	(D ₆)Acetone	93 : 7
	Me ₃ SiO	SbF ₆	(D ₆)Acetone	92 : 8
	Me ₃ SiO	Al[OC(CF ₃) ₃] ₄	(D ₆)Acetone	92 : 8

^a) (*R*)-Configuration at C(2).

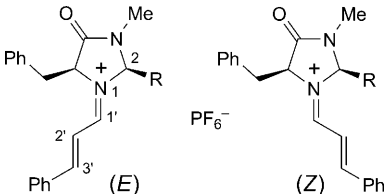
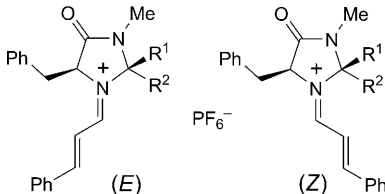
preference, which is evident from *Figs. 4, 5,a*, and *6,a*, for the formation of a thermodynamically less stable cinnamoylidene-imidazolidinone (*Z*)-isomer.

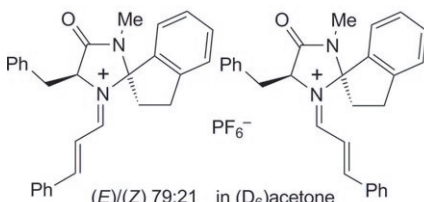
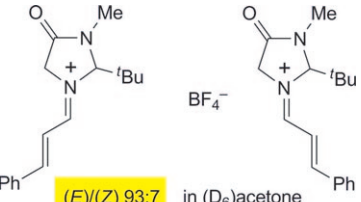
If we make the assumption (*cf. Sect. 5*) that the (*E*)/(*Z*)-geometry of the iminium ion derived from 5-benzyl-2,3-dimethyl-2-phenylimidazolidinone and cinnamaldehyde is determined by the antiperiplanarity of the lone pair at the N-atom and the leaving group H₂O in the intermediate *O*-protonated α -amino alcohol derivative (see center of *Scheme 4*), we have to compare the various approach trajectories of the trigonal centers¹⁶⁾, that lead to these intermediates (*Scheme 4*, top and bottom). Of the two diastereotopic approaches of N(1) on the less sterically encumbered face (Me–C(2)/H–C(5) *vs.* Ph–C(2)/PhCH₂–C(5)) of the imidazolidinone to the *Re*- and *Si*-face of cinnamaldehyde, the *Re*-approach, leading to the (*Z*)-precursor, appears to be more favorable (*cf.* the two labeled arrangements in *Scheme 4*, top left and bottom right).

5. An (*E*)/(*Z*)-Dilemma in Organocatalysis with Diarylprolinol and Imidazolidinone Derivatives? – The results described in the previous sections, which are supported by theory [12][13][15][16][17b][25], must be considered strong evidences for the formation of both (*E*)- and (*Z*)-iminium ions in reactions between enals and the organocatalysts with secondary amino groups. Not only are the two diastereoisomers formed from their precursors, but they are in equilibrium with each other at ambient temperatures in various solvents. Activation barriers are low enough to observe interconversions down to temperatures of –30°.

¹⁶⁾ For a topological rule for the coupling of trigonal centers, see [24].

Table 3. (*E*)/(*Z*) Ratios of the Iminium Hexafluorophosphate Salts **F** and **G** (imidazolidinones derived from (*S*)-phenylalanine) in Solution (determined by ¹H-NMR analysis at ambient temperatures). For details of assignment, see Footnote 13

					
R	(<i>E</i>)/(<i>Z</i>) Ratio in (D ₆)acetone	R ¹	R ²	Solvent	(<i>E</i>)/(<i>Z</i>) Ratio
H	31 : 69	Me	Me	(D ₆)DMSO	98 : 2 ^a
Et	79 : 21	Me	CH ₂ F	(D ₆)Acetone	> 99 : 1
ⁱ Pr	87 : 13	FCH ₂	Me	(D ₆)Acetone	> 99 : 1
^t Bu	95 : 5 ^b	Me	ⁱ Pr	(D ₆)Acetone	> 99 : 1
Ph	67 : 33	ⁱ Pr	Me	(D ₆)Acetone	> 99 : 1
(<i>E</i>)-Et-CH=C(Me)	65 : 35	^t Bu	Me	(D ₆)DMSO	> 99 : 1
(<i>E</i>)-Ph-CH=CH	72 : 28	Me	Ph	(D ₆)DMSO	89 : 11
		Ph	Me	(D ₆)Acetone	76 : 24

			
(E)/(Z) 79:21 in (D ₆)acetone		(E)/(Z) 93:7 in (D ₆)acetone	

^a) Ratio in CD₃CN: 97 : 3; ratio of BF₄⁻ salt in (D₆)acetone: 93 : 7. ^b) Ratio in CD₃CN: 90 : 10.

^a) Ratio in CD₃CN: 97 : 3; ratio of BF₄[−] salt in (D₆)acetone: 93 : 7. ^b) Ratio in CD₃CN: 90 : 10.

From some of the NMR experiments described in Figs. 2–7, a rather slow (*E*)/(*Z*)-interconversion rate can be derived by a rough kinetic analysis. This may be deceiving in view of the conditions under which the actual organocatalysis reactions are conducted; the mechanism of (*E*)/(*Z*) interconversion involves nucleophilic attack on or deprotonation of the iminium ions (*vide infra*)¹⁴; in two of our experiments (Figs. 2 and 3), there is no nucleophile besides possible impurities in the solvent; in the other cases (Figs. 4–7), there is just the water of reaction that could possibly act as nucleophile.

According to the (*E*)/(*Z*) ratios at equilibrium observed at room temperature, which range from 88:12 to 98:2 for the cinnamaldehyde derivatives of typical organocatalysts (see Tables 2 and 3), the free enthalpy differences $\Delta\Delta G^\circ_f$ between the two stereoisomers are 1.5 to 2.5 kcal/mol. If the (*E*)- and (*Z*)-forms would react with a given nucleophile at the same rate, the enantiomer ratios (er) in the products would be the same as the diastereoisomer ratios (dr) of the iminium ions, and thus the enantiomer excesses (ee) should be in the range of 75 to 95% (Fig. 8). This is in

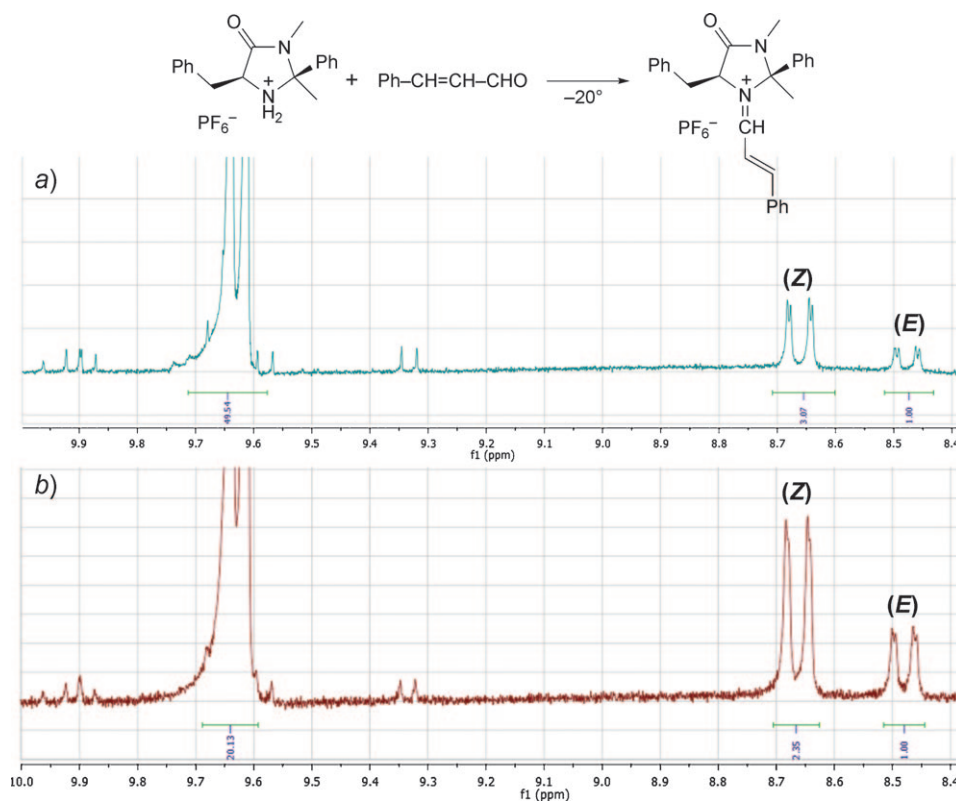


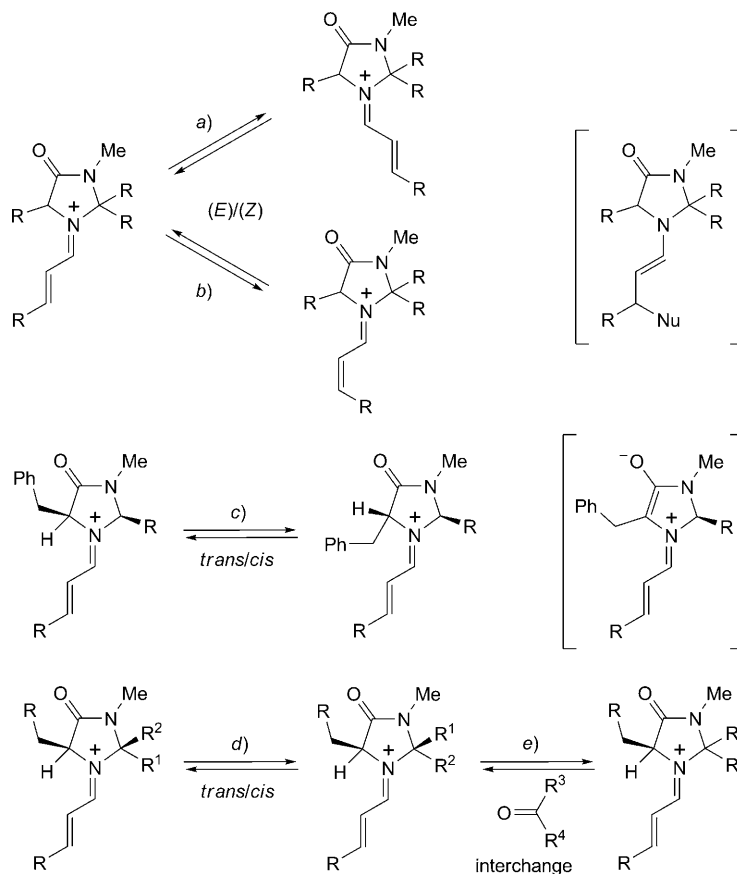
Fig. 4. NMR Spectra resulting from an equimolar mixture of an imidazolidinonium hexafluorophosphate and cinnamaldehyde at -20° in CD_3CN ($4.7 \cdot 10^{-5}$ M solution). a) Spectrum recorded after 30 min; ca. 7% conversion to the iminium ions. b) Spectrum recorded after 20 h; ca. 15% conversion to the iminium ions. For (E)/(Z)-assignment, see Fig. 5, a. The signal at 9.65 ppm is the doublet of the formyl H-atom.

contrast to the frequently observed [3][5][8][13][18][26] or values of up to 99.5:0.5.¹⁷⁾

In the generally accepted mechanistic model, it is assumed that the sterically more favorable (*E*)-iminium ions undergo nucleophilic attack from the face of the π -system, which is *anti* to the large substituent(s) on the heterocycle, in agreement with the observed stereochemical outcome of reactions (Fig. 8, a). With the (*Z*)-iminium ion, the preference for this trajectory should be even greater, leading to the enantiomer of the observed major product (Fig. 8, b). In an equilibrating mixture of (*E*)- and (*Z*)-

¹⁷⁾ The especially high enantioselectivities observed in domino reactions [8] must not be considered in this context, because there is more than one diastereoisomeric transition state in a sequence of reactions involving catalyst derivatives. This can lead to augmentations of the overall enantioselectivities, with which the final products are formed.

Scheme 3. Possible Isomerizations and Interconversions of Iminium Ions Derived from Imidazolidinones and α,β -Unsaturated Aldehydes. a), b) (*E*)/(*Z*)-Isomers with respect to the N=C and C=C bond of enoylidene iminium ions can equilibrate through an enamine intermediate (cf. Footnotes 12 and 14)). c) Epimerization at C(5) of an iminium ion through a zwitter-ionic intermediate; the known higher stability of analogous *cis*- vs. *trans*-1-acyl-imidazolidinones suggests that the equilibrium lies on the side of the *cis*-isomer (see the discussion in [11]). d) Epimerization at C(2) has been observed upon reaction of imidazolidinones with electrophiles (see the discussion in [11]). e) Incorporation of an added carbonyl compound into the heterocycle (see Scheme in [15a]).



iminium ions, which are formed at different rates, the situation becomes more complex¹⁸⁾, as outlined in Scheme 5: If the formation of the iminium ions from enals

¹⁸⁾ An additional degree of complexity has just been added: there is a negative nonlinear effect in the *Michael* addition of dibenzyl malonate to cinnamaldehyde, catalyzed by diphenylprolinol (*tert*-butyl)(dimethyl)silyl ether; this is interpreted as the involvement of a second catalyst molecule, which acts as counter ion $^*\text{R}_2\text{NH}_2^+$ of $(\text{BnOCO})_2\text{CH}^-$, when the iminium ion $^*\text{R}_2\text{N}=\text{CH}-\text{CH}=\text{CHPh}^+$ undergoes nucleophilic attack [20].

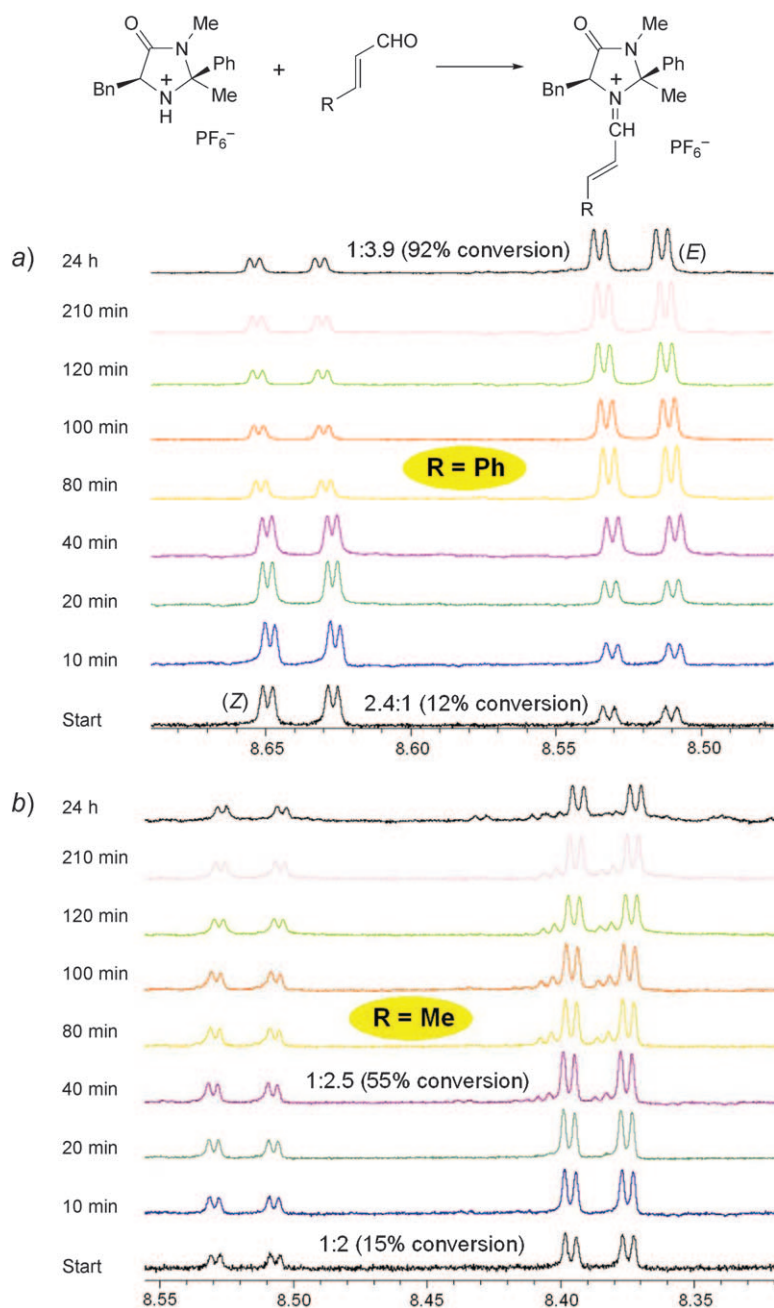


Fig. 5. Low-field section of the 500-MHz ^1H -NMR spectra in CD_3CN of the reaction mixtures containing cinnamaldehyde (a), crotonaldehyde (b), or hex-2-enal (c), and *cis*-(5*S*)-5-benzyl-2,3-dimethyl-2-phenylimidazolidinonium hexafluorophosphate (ambient temperature, molar ratio aldehyde/imidazolidinone 2 : 1). For case a), the signals of $\text{H}-\text{C}(1')$ of (*E*)- and (*Z*)-isomer are shown; assignment by NOEs for (*E*)-form: between $\text{H}-\text{C}(1')$ and Me and between $\text{H}-\text{C}(2')$ and CH_2 , as well as $\text{H}-\text{C}(5)$, for (*Z*)-form: between $\text{H}-\text{C}(1')$ and CH_2 .

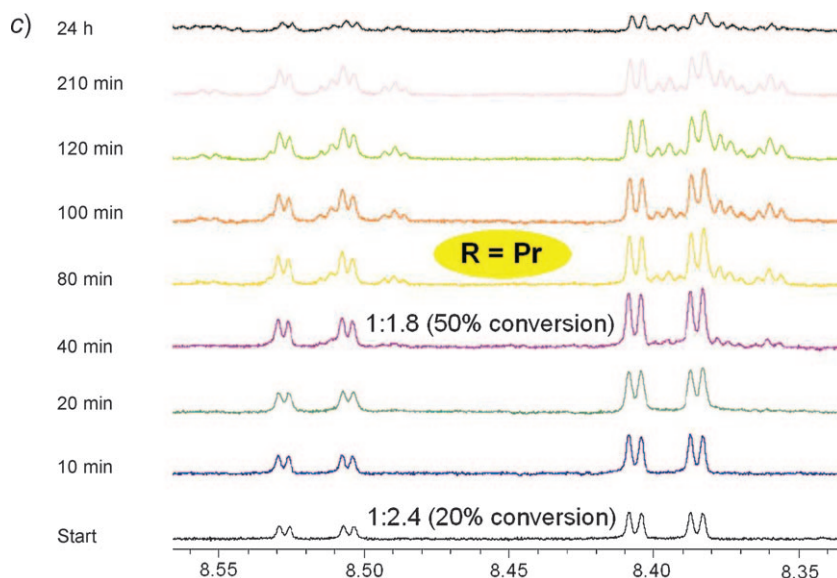


Fig. 5 (cont.)

and ammonium salts is assumed to be irreversible (*Step a* in *Scheme 5*; cf. *Scheme 4*), there are two extreme scenarios: *i*) If the (*E*)/(*Z*)-equilibrating rate (K_{eq} ; *Step b*) is much slower than the rate of reaction with a nucleophile¹⁹⁾ (*Step c*), the enantiomer ratio (er) in the isolated product will be determined by the relative rate of (*E*)/(*Z*)-iminium-ion formation and the respective preference of Nu^{anti} and Nu^{syn} approach to the (*E*)/(*Z*)-diastereoisomeric iminium ions (*Fig. 8*); with exclusive Nu^{anti} attack, er would be equal to k_E/k_Z . *ii*) If, on the other hand, the (*E*)/(*Z*)-equilibrating rate (*Step b*) is much faster than the rate of reaction with a nucleophile (*Step c*), and if there is exclusive Nu^{anti} approach, the system would be subject to the *Curtin–Hammett* principle, and the product er would be equal to $[E]k'_E/[Z]k'_Z$. Scenario *i* is, for instance, not compatible with the *MacMillan* generation-one catalyst: there is *ca.* 25% (*Z*)-iminium ion at the beginning of the reaction with cinnamaldehyde, with rapid equilibration to the (*E*)-form at room temperature (*Fig. 6, a*); the er values observed with this catalyst in addition to α,β -unsaturated aldehydes are in the range of the (*E*)/(*Z*)-equilibrium ratio (98:2 in DMSO, 97:3 in MeCN; see *Table 3* and *Fig. 6, a*). Moreover, when *Jørgensen's* catalyst is used in conjugate additions, the product er values are often above 97:3, while the (*E*)/(*Z*)-equilibrium ratio of the cinnamaldehyde-derived iminium ion is *ca.* 92:8. It should also be mentioned in this context that the [fluoro(diphenyl)methyl]pyrrolidine catalyzes epoxidations (H_2O_2/H_2O) of cinna-

¹⁹⁾ The reaction of iminium triflates (trifluoromethanesulfonates) from cinnamaldehyde and diphenylprolinol trimethylsilyl ether or benzyl-trimethyl-imidazolidinone with silylketene-acetals is very fast: $7 \cdot 10^1 - 9 \cdot 10^3 [M^{-1} s^{-1}]$ [14].

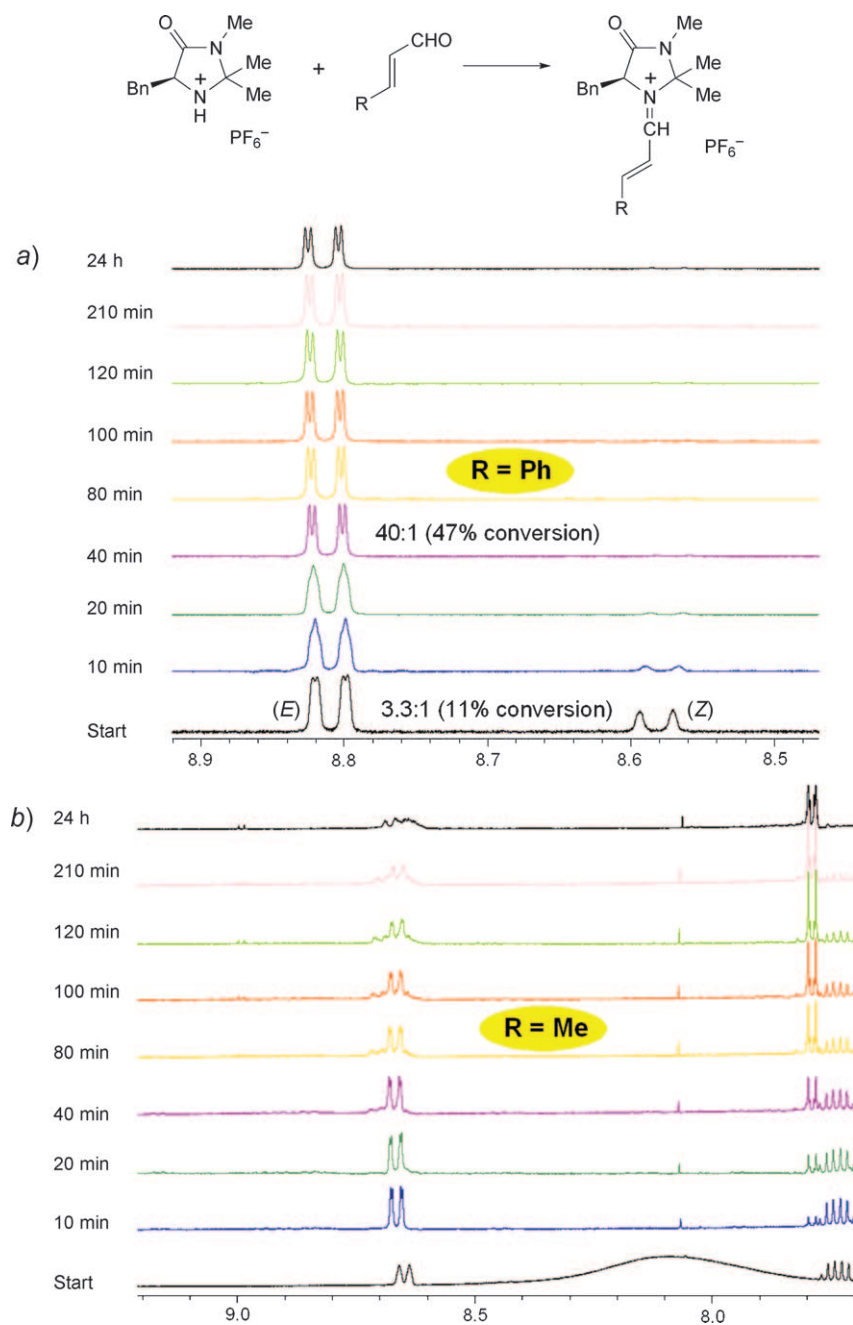


Fig. 6. Low-field section of the 500 MHz ^1H -NMR spectra in CD_3CN of the reaction mixtures containing cinnamaldehyde (a), crotonaldehyde (b), or hex-2-enal (c), and 5-benzyl-2,2,3-trimethylimidazolidinium hexafluorophosphate (ambient temperature, molar ratio aldehyde/imidazolidinone 2:1). For case a), the signals of $\text{H}-\text{C}(1')$ of (*E*)- and (*Z*)-form are shown; assignment of (*E*)-configuration by NOEs between $\text{H}-\text{C}(1')$ and the H-atoms of the geminal Me groups, and between $\text{H}-\text{C}(2')$ and CH_2 , as well as $\text{H}-\text{C}(5)$. Equilibrium ratio (*E*)/(*Z*) = 97:3.

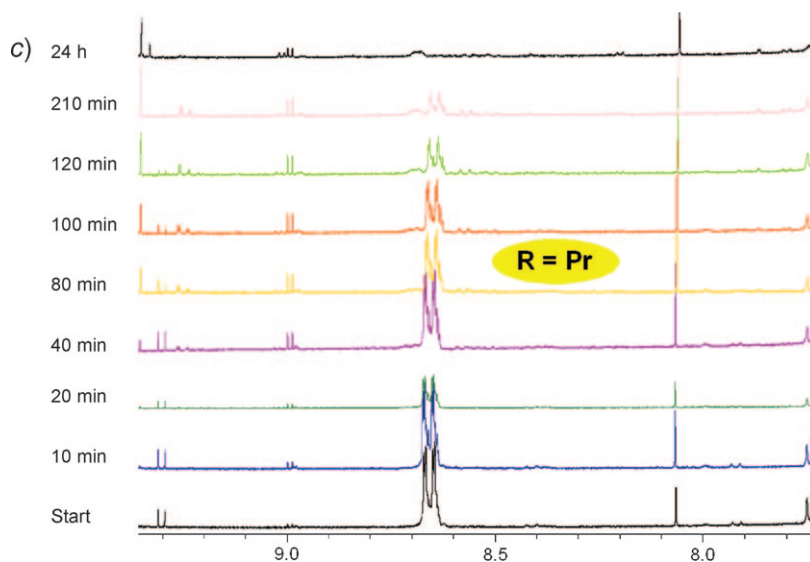


Fig. 6 (cont.)

maldehydes, under a variety of conditions, to give *trans*-2-aryl-oxirane-carbaldehydes with *er* values between 94 : 4 and 98 : 2, while the (*E*)/(*Z*)-iminium ion ratio is *ca.* 9 : 1 in this case [13] (*Scheme 2* and *Table 2*)²⁰.

One conclusion from these observations may be that the (*E*)-isomers of the iminium ions react faster with nucleophiles than the (*Z*)-isomers under equilibrating conditions (*vide supra*, scenario *ii*). What could be the reason of such a potential reactivity difference?²¹

Since the nucleophiles approach the β -C-atoms of the enoylidene iminium ions in an area of space, far away from the sterically demanding groups in 2- or 2,5-positions of the heterocycles, no notable reactivity differences could, at first sight, be expected between (*E*)- and (*Z*)-isomers (*Fig. 8, a* and *b*, left). On the other hand, there will be

²⁰) The *er* value of the minor *cis*-product is unknown. If the topicity of the primary addition of H₂O₂ to the iminium ion would be the *er*-determining step to give an enamine intermediate that can cyclize to either *trans*- or *cis*-product, the diastereoisomeric oxiranes would have the same enantiomer purity.

²¹) One possibility that we have considered is that the ⁺N=C–C=C conjugation and, thus, the electrophilicity of the β -C-atom is reduced in the (*Z*)-form by out-of-plane rotation around the single bond, induced by the substituent in the 2-position of the heterocycle. Inspection of the X-ray structures of (*Z*)-isomers (*Table 1*) and of density functional theory (DFT)-calculated structures of (*Z*)-geometry revealed that there is no fundamental difference in the ⁺N=C–C=C torsion angles for (*E*)- and (*Z*)-isomers; all angles are in the same range, between 175 and 179°.

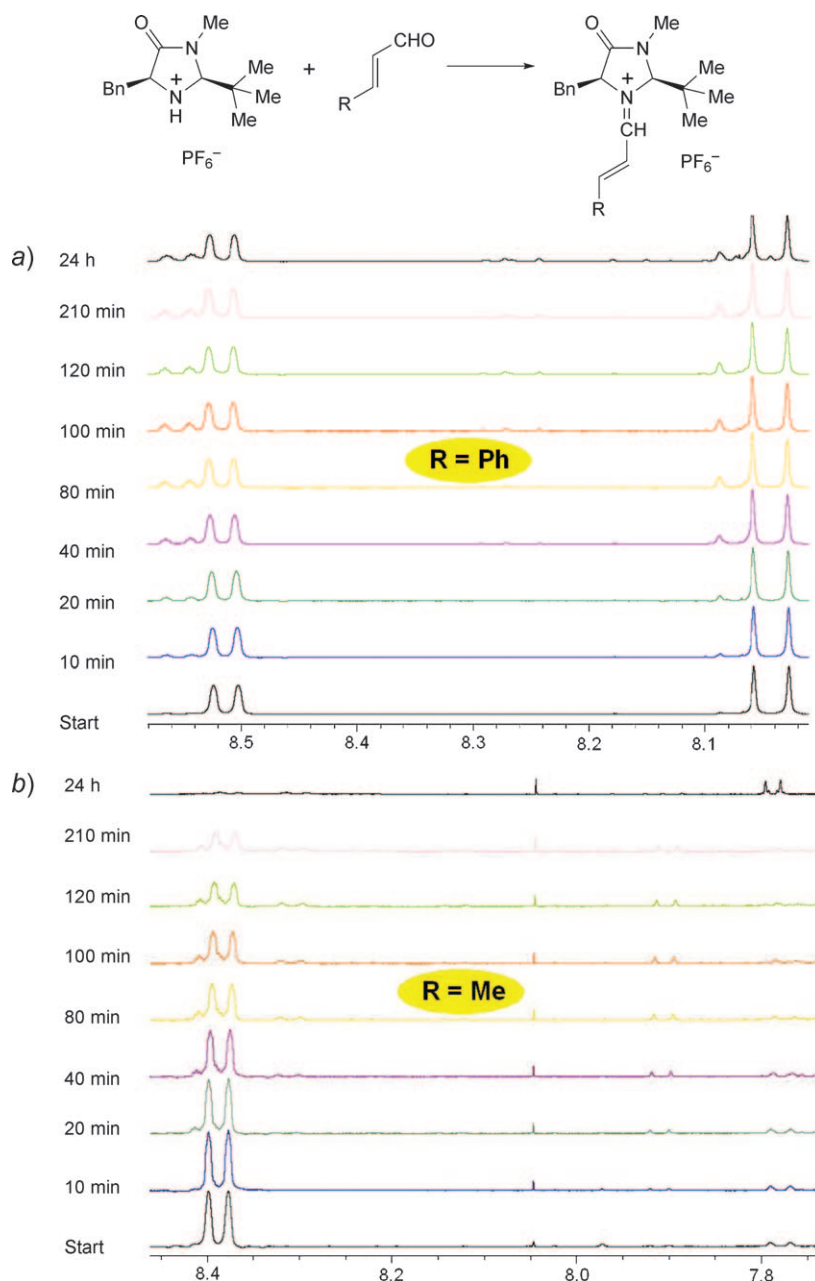


Fig. 7. Low-field section of the 500 MHz ¹H-NMR spectra in CD₃CN of the reaction mixtures containing cinnamaldehyde (a), crotonaldehyde (b), or hex-2-enal (c), and *cis*-5-benzyl-2-(*tert*-butyl)-3-methyl-imidazolidinonium hexafluorophosphate (ambient temperature, molar ratio aldehyde/imidazolidinone 2 : 1). For case a), the signals of H-C(1') at 8.51 ppm and of H-C(3') at 8.04 ppm are shown; both belong to the (*E*)-form, due to NOEs between H-C(1') and the *t*Bu H-atoms, as well as H-C(2), and between H-C(2') and H-C(5). Equilibrium ratio (*E*)/(*Z*) 90 : 10.

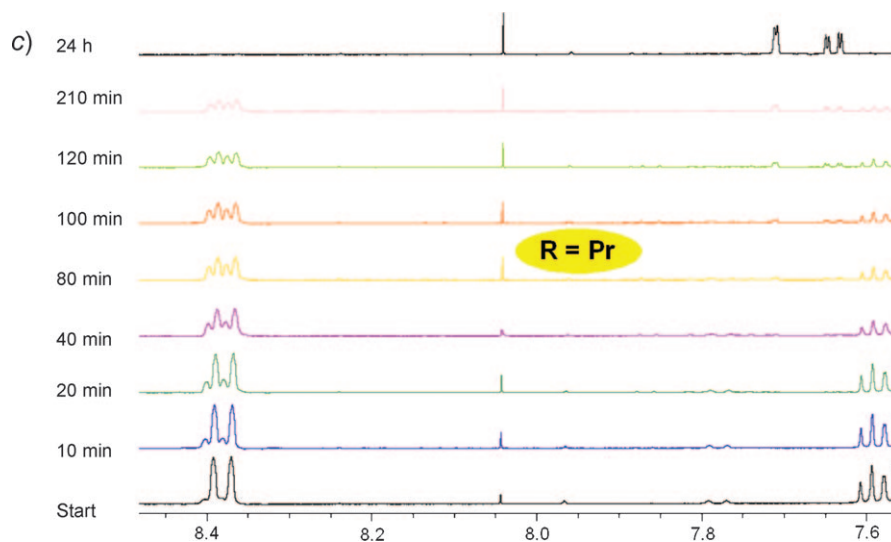
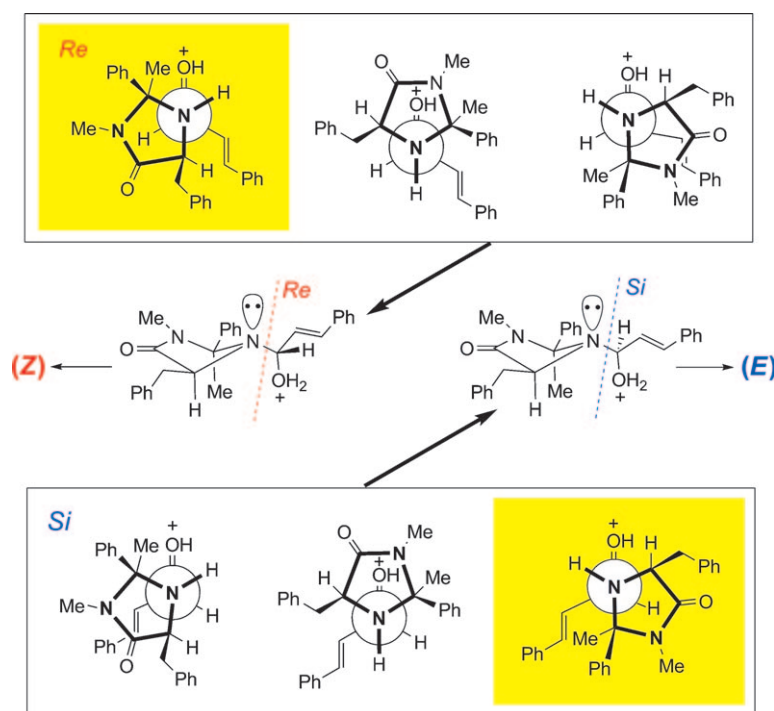


Fig. 7 (cont.)

 Scheme 4. Approach of *N*(1) of *cis*-(5*S*)-5-Benzyl-2,3-dimethyl-2-phenylimidazolidinone to the Carbonyl Re- and Si-Face of Cinnamaldehyde, Leading to (*Z*)- and (*E*)-Iminium Ion, Respectively


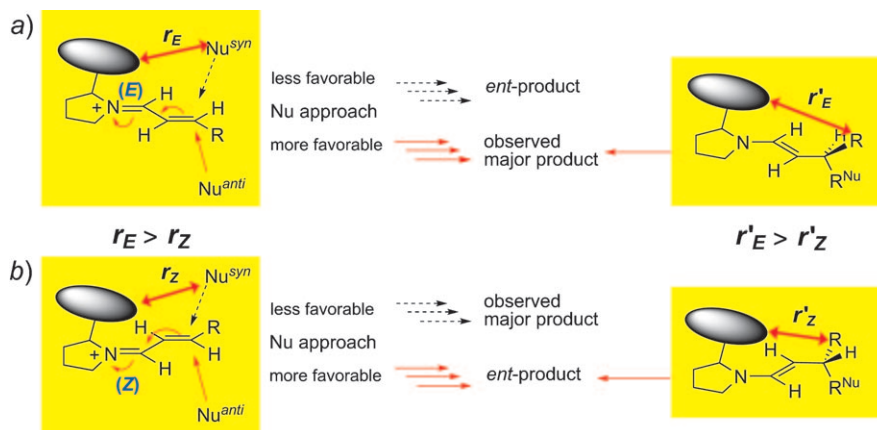


Fig. 8. Trajectories of nucleophilic approaches to the a) (E)- and b) (Z)-enoylidene iminium ions. As demonstrated with the primary adducts' structural Formulae on the right side, more steric repulsion between the R group and a large substituent on the heterocycle is expected to develop on the way to the transition state of the *anti*-approach to the (Z)-ion. In a cycloaddition reaction, the α - and the β -C-atom will pyramidalize.

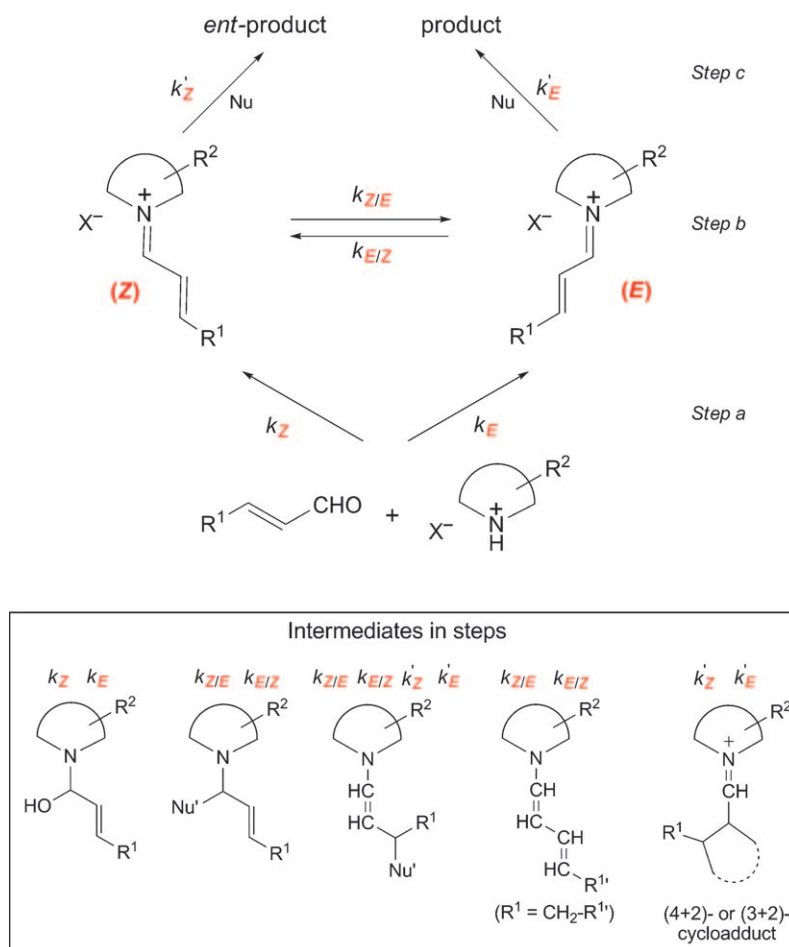
pyramidalization of the acceptor trigonal C-atom on the way to the transition state of nucleophilic attack from the *anti*-side, pushing the substituent R at this C-atom up; as demonstrated by the drawings of the corresponding products on the right side of Fig. 8, a and b, this might be expected to cause more repulsive interactions with the – remote – large substituent on the heterocycle in the case of the (Z)- than in the case of the (E)-iminium precursor.

There is another intriguing possible effect that could cause a rate difference of nucleophilic approach to the *anti*-face of (E)- and (Z)-enoylidene-iminium ions.

We recalled the general observation that the steric course of organic reactions tends to reverse as we go from the 'simple' to the 'vinylogous' structures: S_E2 vs. S_E2' , S_N2 vs. S_N2' , $E2$ vs. $E2'$, butadiene vs. hexatriene cyclization and reversal, etc. (see the discussions (with extensive references) involving the terms 'orbital symmetry correlations' (pericyclic reactions, Woodward–Hoffman rules [27]) 'Hückel/Möbius aromaticity' [28], 'principle of orbital distortions' or ' σ,π interaction' [29], 'alternate motion of electron pairs' [30], 'Boolean alternation' or 'parity of stereochemistry' [31], ' τ -bond or bent-bond model of the C,C double bond' [32]²²). Some examples are outlined in the Appendix. For the addition to iminium ions and conjugate addition to 'vinylium' ions, the application of these principles would lead to the expectation that the direction of N-pyramidalization might be reversed (Fig. 9). This would mean that, upon approach of a nucleophile, the C-atom attached to the iminium N-atom

²²) This is by no means a complete list of terms and references. The authors assume the responsibility for having omitted further seminal contributions on this subject.

Scheme 5. Simplified Kinetic Scheme of the Formation and Reaction of the Intermediate Iminium Ions from an α,β -Unsaturated Aldehyde and a Chiral Cyclic Amino Compound. A selected number of possible intermediates in the various steps are shown in the box on the bottom. For discussions of the kinetics and stereochemistry, see accompanying text, Scheme 4, and Figs. 8 and 9.



would move down towards the nucleophile, out-of-plane of the original π -system, in the 'simple' case (A_N in Fig. 9,a), in reversal of the elimination of a leaving group with formation of the iminium bond (E in Fig. 9,a; cf. Scheme 4, center). Conversely, in the 'vinylogous' case, pyramidalization would occur in the opposite direction, *i.e.*, such that the C-atom with its 'substituent' moves up, out of the plane of the original π -system (\equiv average plane of the five-membered ring heterocycle, see Fig. 9,b). For the (Z)-isomer of the enoylidene iminium ions, this movement would push the entire substituent at the N-atom towards the sterically demanding group on the heterocycle, causing more 'steric stress' than in the case of the (E)-isomer. This is especially true for

the diarylprolinol derivatives (having *no* substituent at C(5) of the pyrrolidine ring) and for the imidazolidinones with a ^tBu group at C(2) (see Fig. 9, *c*)²³).

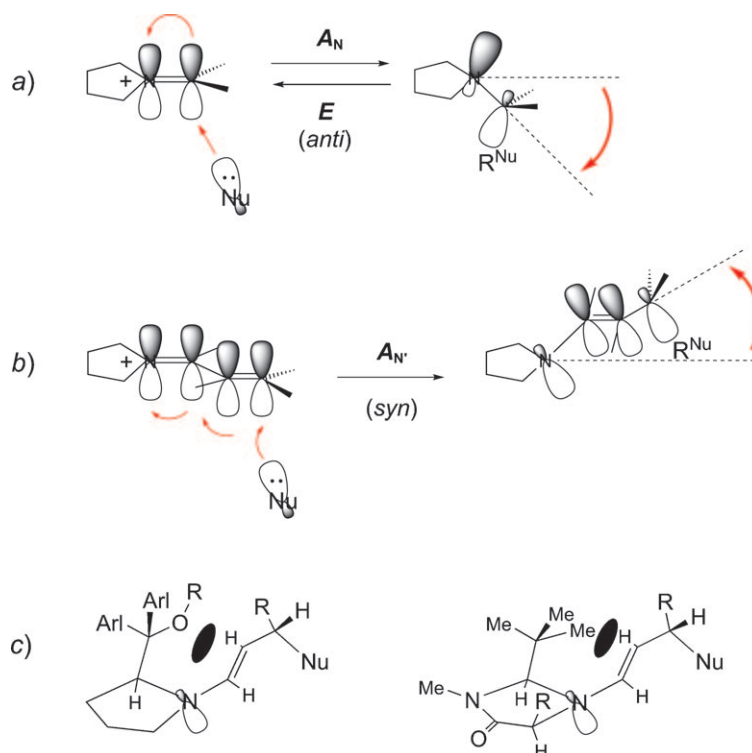
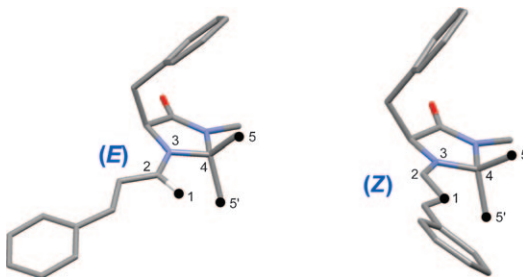


Fig. 9. Possible reversal of the stereochemical course of direct (*a*) and conjugate addition (*b*) of a nucleophile to an iminium ion and an α,β -unsaturated iminium ion, respectively, and 'steric stress' thus arising in the course of nucleophilic approach to (*Z*)-iminium ions derived from a diarylprolinol or a 2-^tBu-imidazolidinone (*c*)

²³) For the 2,2-dimethyl-substituted imidazolidinone (MacMillan's 'first-generation catalyst' [4b]), it is not so obvious at first sight, why the upward movement of the substituent at N(1), as outlined in Fig. 9, should cause more 'steric stress', when it occurs with the (*Z*)-, rather than the (*E*)-iminium ion. However, when we look at models of the two diastereoisomeric ions, we realize that movement of the substituent at the N-atom (up or down) will cause stronger *1.5-repulsion* [33] in the (*Z*)- (CH/Me) than in the (*E*)-form (H/Me) (cf. Fig. 13 in [11]).



6. DFT Calculations of Heterosubstituted Enamine Model Compounds. – We first calculated the (*E*)/(*Z*)- and *s-trans*/*s-cis*-energy differences of the simple diarylprolinol derivatives shown in Fig. 10. Comparison of the values suggests that attack of HO[−] to (*E*)- and (*Z*)-iminium ions has approximately the same exothermicity²⁴). In the optimized geometries, the N-atoms have a small degree of pyramidalization in the direction of the large substituent at C(2) of the pyrrolidine ring, in agreement with all previously calculated [12][15b][16][17b][25] and measured [12][15][16] structures.

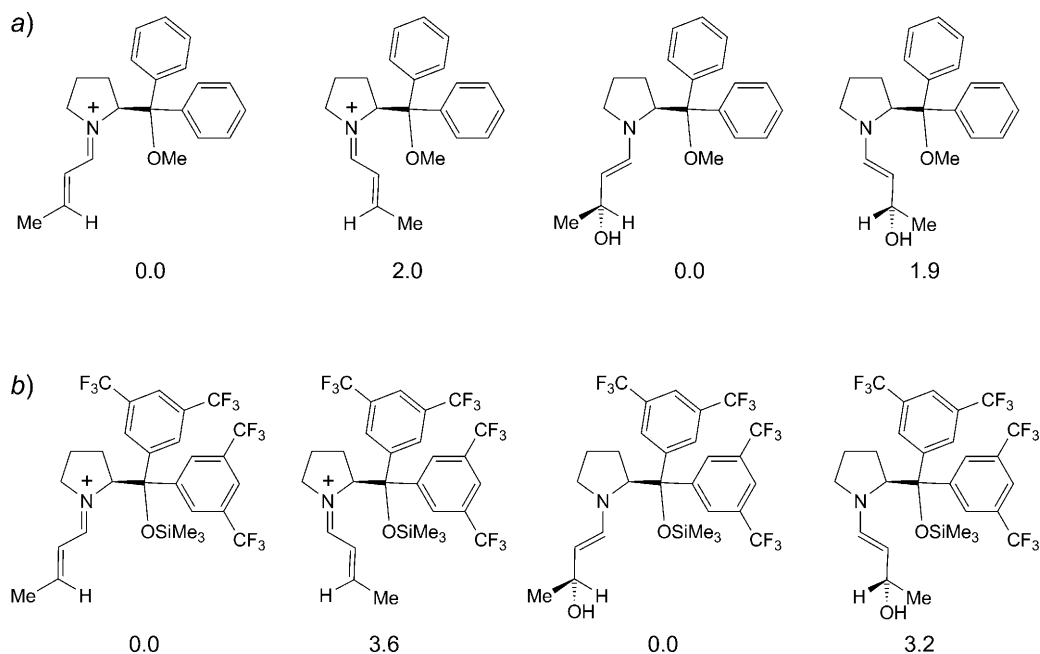


Fig. 10. DFT-Calculated relative energies [kcal/mol] of (*E*)/(*Z*)-iminium ions and of the corresponding *s-trans*/*s-cis*-hydroxyenamines derived from crotonaldehyde and diarylprolinol ethers. In all cases, the more stable *sc-exo*-conformation [11][12] around the exocyclic C,C bond was used for the calculations. a) Diphenylprolinol-methyl-ether derivatives; the energies are the sum of potential energy + zero-point energy; approximately the same results were obtained with geometry optimizations at MPB1K/6-31 + G(d,p) or PBE1PBE/6-31 + G(d,p) levels. b) Relative potential energies of the compounds derived from Jørgensen's catalyst with geometry optimizations at B3LYP/6-31G(d) level; the energy differences between the (*E*)- and (*Z*)-isomers are 3.64 and 2.92 kcal/mol for the iminium ions and the hydroxy enamines, respectively. Similar values are obtained (3.36 and 3.89 kcal/mol for the iminium ions and 3.45 and 3.19 kcal/mol for the hydroxy enamines) with the subsequent single-point energy evaluations at computational levels of MPWB1K/6-31 + G(d,p) and PBE1PBE/6-31 + G(d,p), respectively.

²⁴⁾ Such a reaction in the gas phase has no activation barrier (*cf.* Fig. 13), so that the more exothermic reaction is expected to be faster than the less exothermic one; in the cases presented in Fig. 10, the energy differences between the starting materials ((*E*)/(*Z*)-iminium ions) and between the corresponding products (*s-trans*/*s-cis*-hydroxyenamines) are almost the same, *i.e.*, the exothermicity is the same.

To see whether a change in the pyramidalization direction could be detected by DFT calculations when we go from an α -heterosubstituted amine (for which there is ample evidence of virtual *antiperiplanar* (*ap*) arrangement of the lone-pair and the C–X bond; see **H** in Fig. 11, and cf. Fig. 9, a, and Scheme 4, center [34]) to the vinylogous structure, we have computed, at the CBS-QB3 level, the simple model **J**, the *trans*-*N,N*-dimethylpropenamine with allylic hetero substituents X = F, OH, SH, Me₃N⁺. For F, OH, and SH, three conformational energy minima were found: **J**_{syn} with the direction of N-pyramidalization *syn* to the C–X bond (cf. Fig. 9, b), **J**_{anti} with the pyramidalization in the opposite direction, and **J**_{ortho} with the C–X bond in the π -plane of the C=C bond (Figs. 11 and 12). In all three cases, the **J**_{syn} conformations are the most stable ones. The energy differences between **J**_{syn} and **J**_{anti} are, however, very small, a tiny < 0.1 kcal/mol, increasing somewhat from F to OH to SH; the **J**_{ortho} conformations are by 1.4 to 1.8 kcal/mol higher in energy; the N-inversion barrier of the F derivative is calculated to be *ca.* 1 kcal/mol; the values are listed in Table 4. The ammonium ion **J**, X = Me₃N⁺, is an exception: only the conformational minimum **J**_{syn} was found. Note that **J**_{syn} corresponds to what is shown in Fig. 9, b.

On the other hand, no difference can be detected, when the hydroxy-enamine conformations **J**_{syn} and **J**_{anti}, X = OH, are dissociated to CH₂=CH–CH=N⁺Me₂ and OH[–], which, in microscopic reversibility, is equivalent to the addition of a OH[–] to the iminium ion: the energy profiles are essentially the same in this anion–cation dissociation/collapse involving large amounts of energy (Fig. 13).

Although the DFT-detected effects are minute, we venture to cautiously compare them with the assumptions made in the previous section about possible reasons for an (*E*)/(*Z*)-reactivity difference of conjugated iminium ions. According to theory, there

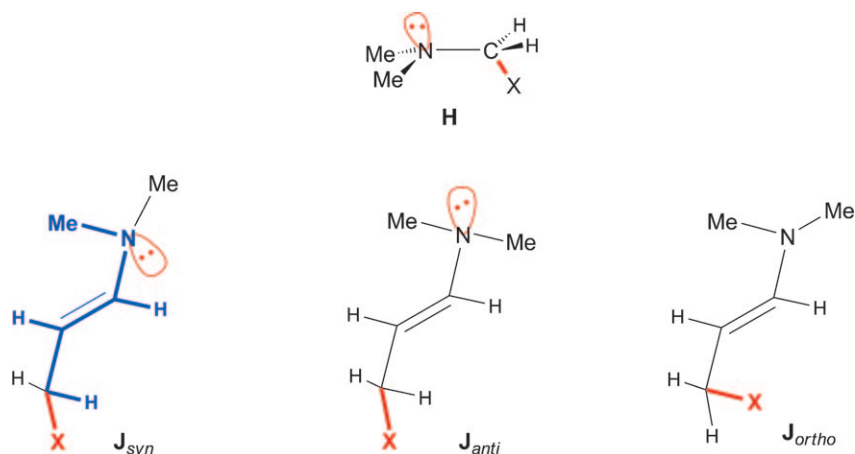


Fig. 11. Conformation of an α -heterosubstituted trimethylamine **H** [34] and DFT-computed conformational minima **J**_{syn}, **J**_{anti}, **J**_{ortho} of the *trans*-*N,N*-dimethyl-enamine derived from β -heterosubstituted propanals (vinylogous to **H**). The blue-labeled atoms and bonds in **J**_{syn} lie approximately in one plane (cf. presentations in Fig. 12); in **J**_{ortho}, the heteroatom X, rather than a H-atom of the X–CH₂ group, resides in this plane. For energies and N-pyramidalizations, see Table 4.

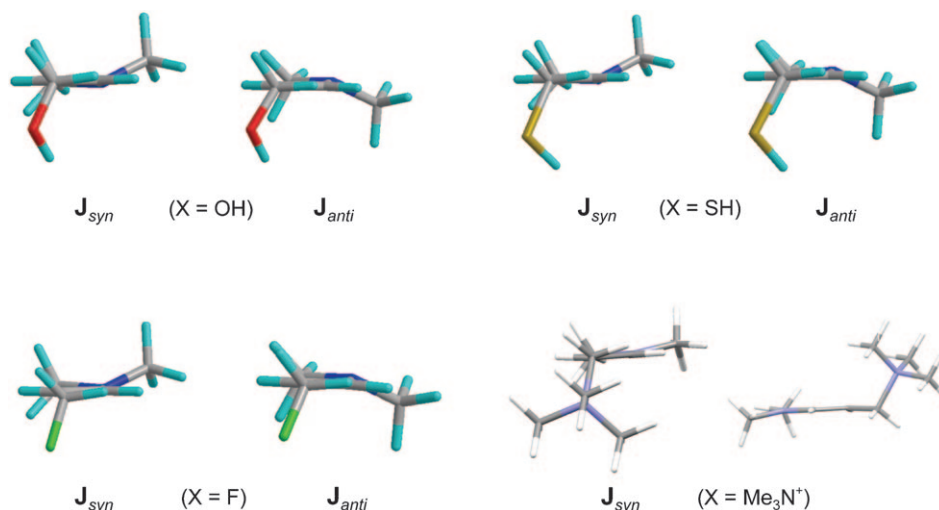


Fig. 12. View along the XH_2C-CH bond of \mathbf{J}_{syn} and \mathbf{J}_{anti} , $X = OH, SH, F$, and Me_3N^+ , and view along the plane of the $CH=CH$ bond in \mathbf{J}_{syn} , $X = Me_3N^+$. Structures computed at the DFT level B3LYP/6-311G(d,p). For relative energies, see Table 4.

appears to be a tiny preference for a reversal of the N-pyramidalization direction, when we compare an α -heterosubstituted amine with a γ -heterosubstituted enamine (cf. Fig. 9, *a* and *b*, with Fig. 12 and Table 4). The fact that only the \mathbf{J}_{syn} form was found with $X = Me_3N^+$ could perhaps be correlated with the fact that neutral, rather ‘soft’ nucleophiles are the preferred reagents²⁵⁾ to attack enoylidene iminium-ion reactive intermediates of the type discussed here, and not F^- , OH^- or HS^- .

7. Conclusions. – The presence of (*E*)/(*Z*)-isomeric iminium ions in organocatalytic applications of diarylprolinol and imidazolidinone derivatives for the activation of α,β -unsaturated aldehydes is most likely due to a dynamic kinetic separation of these diastereoisomers. The reasons of such a reactivity difference, as outlined in Figs. 8 and 9, may not be the only ones²⁶⁾.

We realize that our discussion in Sect. 5 is speculative, full of words like ‘if’, ‘may’, ‘might’, ‘could’, ‘should’, ‘would’, ‘likely’, ‘probably’, ‘potential’, ‘assume’, ‘expect’, ‘suggest’! Also, the DFT calculations described in Sect. 6 hardly provide support for the qualitative discussions, at this point. More elaborate investigations will be necessary to

²⁵⁾ For instance, dienes and heterodienes in *Diels–Alder* reactions, nitrones in (3 + 2)-cycloadditions, pyrroles and indoles in *Friedel–Crafts* reactions, *Hantzsch* ester for hydride transfer, oximes for hydroxylations, hydroxylamine derivatives for amination, etc. [3b][4b][35].

²⁶⁾ We realize that effects of the type discussed here may be small, will depend on the nature of the nucleophiles and of counterions, can be overridden by stronger steric effects and, even more so, by the presence of metal ions (*not* involved in organocatalyses!) (see [29][32c,d]; for a recent theoretical study of the role Li and Na salts may play in S_N2' reactions, see [29c]).

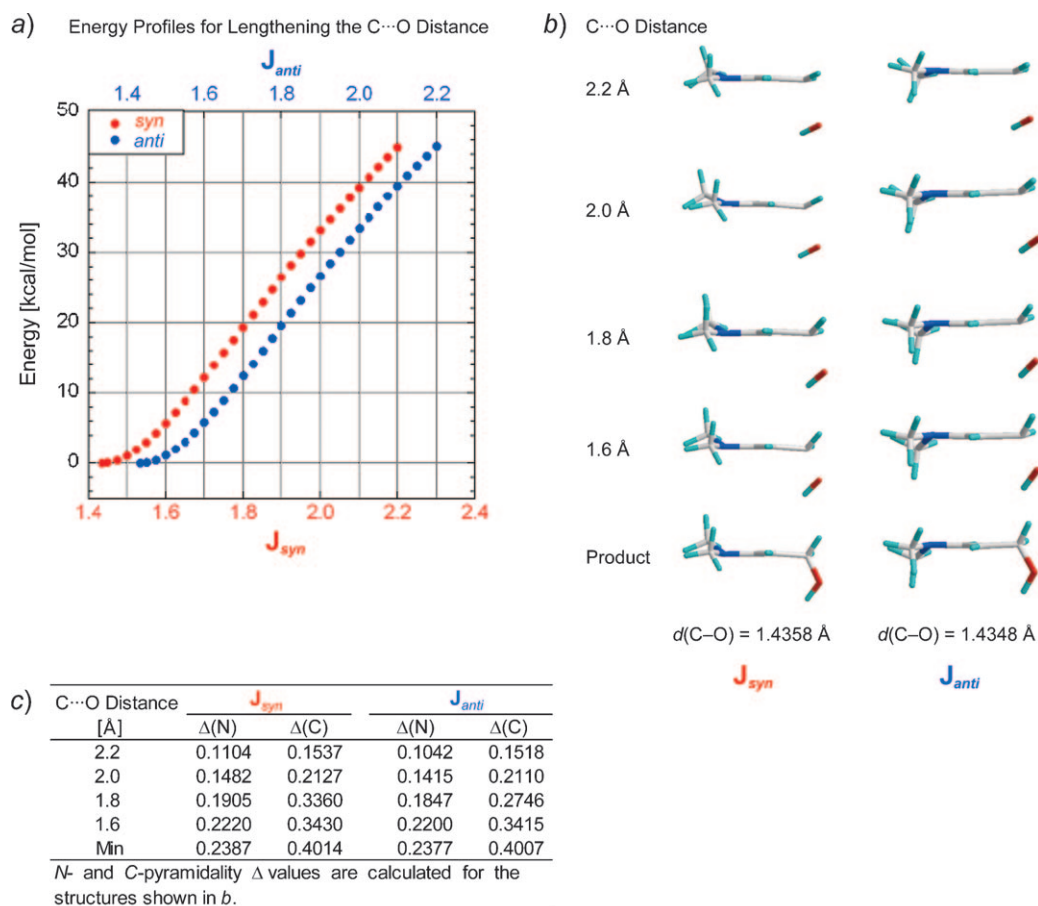


Fig. 13. Energy profiles (a) and intermediate arrangements (b) in the dissociation/formation of J_{syn} and J_{anti} to and from $CH_2=CH-CH=NMe_2^+$ and OH^- , respectively. The pyramidalizations on N and CH_2 increase with decreasing distance of HO^- (c), and the relative direction of pyramidalizations 'syn' (in b, left column) and 'anti' (in b, right column) are retained throughout. The calculation of this anion-cation collapse/dissociation to/of J_{syn} and J_{anti} is not compatible with the view presented in Fig. 9, b.

learn why the fascinating applications of such a simple 'classical' reaction (of amino with carbonyl compounds) work so well. Organocatalysis may thus call mechanistic organic chemists to the fore and lead to a revival of the poorly funded field of physical organic chemistry.

We look forward to critical discussions with colleagues knowledgeable in the fields of organocatalysis, of complex kinetics, of stereoelectronic effects, and of computational theory.

Table 4. *Relative Energies* [kcal/mol] *and* N-Pyramidalization Δ [Å] *of Conformations* \mathbf{J}_{syn} , \mathbf{J}_{anti} , $\mathbf{J}_{\text{ortho}}$ *with* $X = F, OH, SH, Me_3N^+$ (cf. Figs. 11 and 12), *Computed at the CBS-QB3 Level.* E_{pot} = Potential energy; E_{zp} = zero-point energy; E_{TS} = transition-state energy of N inversion; N-pyramid. = pyramidalization of the N-atom; Δ = distance between N and the plane of its three bonding partners; +/– indicates the relationship between the direction of pyramidalization and that of the C,X bond. For the Me_3N^+ -substituted structure, only the \mathbf{J}_{syn} minimum was detected in this calculation.

X		\mathbf{J}_{syn}	\mathbf{J}_{anti}	$\mathbf{J}_{\text{ortho}}$	E_{TS}
F	E_{pot}	0.000	0.024	1.829	1.091
	$E_{\text{pot}} + E_{\text{zp}}$	0.000	0.022	1.705	0.743
	N-pyramid. Δ	+ 0.212	– 0.218		
OH	E_{pot}	0.000	– 0.031	1.653	
	$E_{\text{pot}} + E_{\text{zp}}$	0.000	– 0.042	1.677	
	N-pyramid. Δ	+ 0.239	– 0.238		
SH	E_{pot}	0.000	0.083	1.496	
	$E_{\text{pot}} + E_{\text{zp}}$	0.000	0.063	1.368	
	N-pyramid. Δ	+ 0.244	– 0.243		
Me_3N^+	N-pyramid. Δ	+ 0.076			

The help of P. Zumbrennen in recording NMR spectra (NMR service unit of the LOC) is gratefully acknowledged.

REFERENCES

- [1] W. Langenbeck, 'Die organischen Katalysatoren und ihre Beziehungen zu den Fermenten', Julius Springer, Berlin, 1935.
- [2] J. von Liebig, *Liebigs Ann. Chem.* **1860**, 113, 1.
- [3] a) B. List, R. A. Lerner, C. F. Barbas III, *J. Am. Chem. Soc.* **2000**, 122, 2395; b) K. A. Ahrendt, C. J. Borths, D. W. C. MacMillan, *J. Am. Chem. Soc.* **2000**, 122, 4243.
- [4] a) C. F. Barbas III, *Angew. Chem.* **2008**, 120, 44; *Angew. Chem., Int. Ed.* **2008**, 47, 42; b) D. W. C. MacMillan, *Nature* **2008**, 455, 304; G. Lelais, D. W. C. MacMillan, 'History and Perspectives of Chiral Organic Catalysts', in 'New Frontiers in Asymmetric Catalysis', Eds. K. Mikami, M. Lautens, John Wiley & Sons, Hoboken, 2007, pp. 313; c) B. List, *Angew. Chem.* **2010**, 122, 1774; *Angew. Chem., Int. Ed.* **2010**, 49, 1730.
- [5] J. Franzén, M. Marigo, D. Fielenbach, T. C. Wabnitz, A. Kjærsgaard, K. A. Jørgensen, *J. Am. Chem. Soc.* **2005**, 127, 18296; Y. Hayashi, H. Gotoh, T. Hayashi, M. Shoji, *Angew. Chem.* **2005**, 117, 4284; *Angew. Chem., Int. Ed.* **2005**, 44, 4212.
- [6] M. P. Sibi, M. Hasegawa, *J. Am. Chem. Soc.* **2007**, 129, 4124; T. D. Beeson, A. Mastracchio, J.-B. Hong, K. Ashton, D. W. C. MacMillan, *Science* **2007**, 316, 582.
- [7] R. E. Ireland, 'Organic Synthesis', Prentice-Hall, Englewood Cliffs, 1969.
- [8] D. Enders, C. Grondal, M. R. M. Hüttl, *Angew. Chem.* **2007**, 119, 1590; *Angew. Chem., Int. Ed.* **2007**, 46, 1570; D. Enders, M. R. M. Hüttl, G. Raabe, J. W. Bats, *Adv. Synth. Catal.* **2008**, 350, 267; C. Grondal, M. Jeanty, D. Enders, *Sci. Chem.* **2010**, 2, in print; X. Yu, W. Wang, *Org. Biomol. Chem.* **2008**, 6, 2037.
- [9] B. List, L. Hoang, H. J. Martin, *Proc. Natl. Acad. Sci. U.S.A.* **2004**, 101, 5839.
- [10] a) D. Seebach, A. K. Beck, D. M. Badine, M. Limbach, A. Eschenmoser, A. M. Treasurywala, R. Hobi, W. Prikozovich, B. Linder, *Helv. Chim. Acta* **2007**, 90, 425; b) C. Isart, J. Burés, J. Vilarrasa, *Tetrahedron Lett.* **2008**, 49, 5414.
- [11] D. Seebach, U. Grošelj, D. M. Badine, W. B. Schweizer, A. K. Beck, *Helv. Chim. Acta* **2008**, 91, 1999.
- [12] U. Grošelj, D. Seebach, D. M. Badine, W. B. Schweizer, A. K. Beck, I. Krossing, P. Klose, Y. Hayashi, T. Uchimaru, *Helv. Chim. Acta* **2009**, 92, 1225.

- [13] C. Sparr, W. B. Schweizer, H. M. Senn, R. Gilmour, *Angew. Chem.* **2009**, *121*, 3111; *Angew. Chem., Int. Ed.* **2009**, *48*, 3065.
- [14] S. Lakhdar, T. Tokuyasu, H. Mayr, *Angew. Chem.* **2008**, *120*, 8851; *Angew. Chem., Int. Ed.* **2008**, *47*, 8723.
- [15] a) U. Großel, W. B. Schweizer, M.-O. Ebert, D. Seebach, *Helv. Chim. Acta* **2009**, *92*, 1; b) D. Seebach, U. Großel, W. B. Schweizer, S. Grimme, C. Mück-Lichtenfeld, *Helv. Chim. Acta* **2010**, *93*, 1.
- [16] J. B. Brazier, G. Evans, T. J. K. Gibbs, S. J. Coles, M. B. Hursthouse, J. A. Platts, N. C. O. Tomkinson, *Org. Lett.* **2009**, *11*, 133.
- [17] a) O. Andrey, A. Alexakis, A. Tomassini, G. Bernardinelli, *Adv. Synth. Catal.* **2004**, *346*, 1147; S. Mossé, O. Andrey, A. Alexakis, *Chimia* **2006**, *60*, 216; b) O. Gutierrez, R. Iafe, K. N. Houk, *Org. Lett.* **2009**, *11*, 4298.
- [18] T. J. Peelen, Y. Chi, S. H. Gellman, *J. Am. Chem. Soc.* **2005**, *127*, 11598.
- [19] N. J. Leonard, J. V. Paukstelis, *J. Org. Chem.* **1963**, *28*, 3021.
- [20] I. Fleischer, A. Pfaltz, *Chem.–Eur. J.* **2010**, *16*, 95.
- [21] ‘Powder Diffraction Theory and Practice’, Eds. R. E. Dinnebier, S. J. L. Billinge, RSC Publishing, Cambridge, 2008.
- [22] ‘Structure Determination from Powder Diffraction Data’, Eds. W. I. F. David, K. Shankland, L. B. McCusker, C. Baele, Oxford University Press, 2002; W. I. F. David, K. Shankland, *Acta Crystallogr., Sect. A* **2008**, *64*, 52.
- [23] C. Baerlocher, A. Hepp, ‘XRS-82: The X-Ray Rietveld System’, Institut für Kristallographie, ETH Zürich, 1982.
- [24] D. Seebach, J. Goliński, *Helv. Chim. Acta* **1981**, *64*, 1413.
- [25] R. Gordillo, J. Carter, K. N. Houk, *Adv. Synth. Catal.* **2004**, *346*, 1175.
- [26] Y. Chi, S. H. Gellman, *Org. Lett.* **2005**, *7*, 4253; Y. Chi, S. H. Gellman, *J. Am. Chem. Soc.* **2006**, *128*, 6804.
- [27] a) R. B. Woodward, R. Hoffmann, *Angew. Chem.* **1969**, *81*, 797; *Angew. Chem., Int. Ed.* **1969**, *8*, 781; b) D. Seebach, *Fortschr. Chem. Forsch.* **1968**, *11*, 177.
- [28] E. Heilbronner, *Tetrahedron Lett.* **1964**, *5*, 1923; H. E. Zimmermann, *J. Am. Chem. Soc.* **1966**, *88*, 1564, 1566.
- [29] a) E. M. Burgess, C. L. Liotta, *J. Org. Chem.* **1981**, *46*, 1703; N. T. Anh, *Chem. Commun.* **1968**, 1089; K. Fukui, H. Fujimoto, *Bull. Chem. Soc. Jpn.* **1966**, *39*, 2116; b) J. T. Koh, L. Delaude, R. Breslow, *J. Am. Chem. Soc.* **1994**, *116*, 11234; c) A. Streitwieser, E. G. Jayasree, F. Hasanayn, S. S.-H. Leung, *J. Org. Chem.* **2008**, *73*, 9426.
- [30] M. L. Dhar, E. D. Hughes, C. K. Ingold, A. M. M. Mandour, G. A. Maw, L. I. Woolf, *J. Chem. Soc.* **1948**, 2093; C. K. Ingold, ‘Structure and Mechanism in Organic Chemistry’, 2nd edn., Cornell University Press, Ithaca, 1969.
- [31] J. Mathieu, A. Rassat, *Tetrahedron* **1974**, *30*, 1753.
- [32] a) K. L. Brown, L. Damm, J. D. Dunitz, A. Eschenmoser, R. Hobi, C. Kratky, *Helv. Chim. Acta* **1978**, *61*, 3108; b) C. E. Wintner, *J. Chem. Educ.* **1987**, *64*, 587; c) E. Vogel, G. Caravatti, P. Franck, P. Aristoff, C. Moody, A.-M. Becker, D. Felix, A. Eschenmoser, *Chem. Lett.* **1987**, 219; d) V. G. Matassa, P. R. Jenkins, A. Kümin, L. Damm, J. Schreiber, D. Felix, E. Zass, A. Eschenmoser, *Isr. J. Chem.* **1989**, *29*, 321; e) S. J. Blarer, D. Seebach, *Chem. Ber.* **1983**, *116*, 2250.
- [33] G. Quinkert, E. Egert, C. Griesinger, ‘Aspekte der Organischen Chemie: Struktur’, Verlag Helvetica Chimica Acta, Basel, 1995; G. Quinkert, E. Egert, C. Griesinger, ‘Aspects of Organic Chemistry: Structure’, Verlag Helvetica Chimica Acta, Basel, 1996.
- [34] P. Deslongchamps, ‘Stereochemical Effects in Organic Chemistry’, Pergamon Press, Oxford, 1983; E. Juaristi, G. Cuevas, ‘The Anomeric Effect’, CRC Press, Boca Raton, 1995; A. J. Kirby, ‘Stereochemical Effects’, Oxford University Press, Oxford, 1996.
- [35] T. B. Poulsen, K. A. Jørgensen, *Chem. Rev.* **2008**, *108*, 2903; A. Dondoni, A. Massi, *Angew. Chem.* **2008**, *120*, 4716; *Angew. Chem., Int. Ed.* **2008**, *47*, 4638; P. Melchiorre, M. Marigo, A. Carlone, G. Bartoli, *Angew. Chem.* **2008**, *120*, 6232; *Angew. Chem., Int. Ed.* **2008**, *47*, 6138; S. Bertelsen, K. A. Jørgensen, *Chem. Soc. Rev.* **2009**, *38*, 2178; P. Merino, E. Marqués-López, T. Tejero, R. P. Herrera, *Synthesis* **2010**, *1*.

Received February 17, 2010

Appendix. – As a didactic contribution intended for students, we have assembled presentations involving concerted bond-forming and bond-breaking processes in *Charts 1–6*. For reaction specifications, we use the *Ingold* nomenclature [30]. As a mnemonic device we use: ‘Reactions involving an odd number of electron pairs form or break bonds in the same half-space; reactions involving an even number of electron pairs form or break bonds in two different spaces’ (*Mathieu and Rassat* [31]). As part of the mnemonic device, the p-lobes in *Charts 1–6* and in *Fig. 9* are used to indicate the half-spaces (dark vs. white lobes); the presentations are *not* to be mixed up with the lowest occupied molecular orbitals of the various π -systems! For actual examples of the various processes and for additional reactions that may be described along these lines (cf. electrophilic 1,4-addition of X–Y to a diene, *Eschenmoser–Grob* fragmentation, etc.) and for critical discussions, we refer the reader to the numerous citations given in [10a] [27–34].

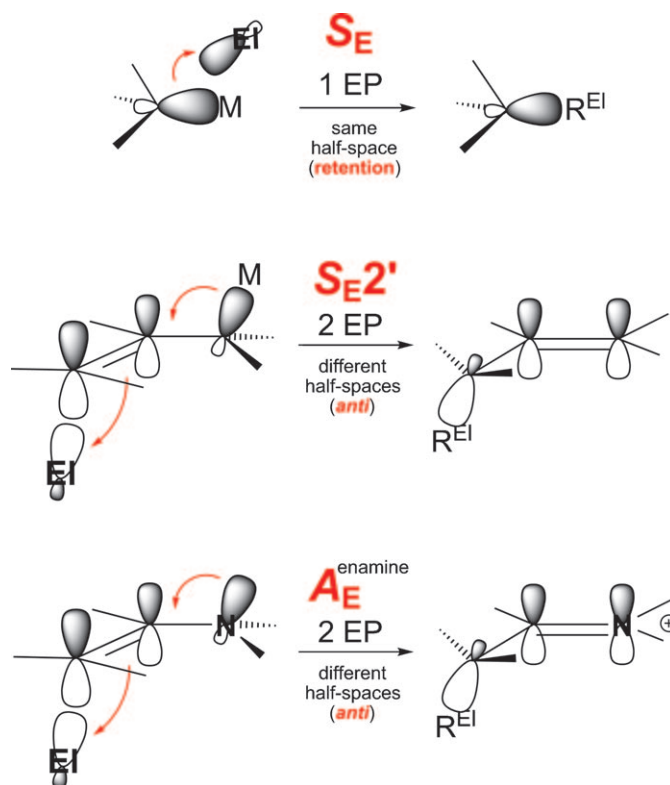


Chart 1. Electrophilic substitutions and the reaction of an enamine with an electrophile, which may be considered an extreme version of an electrophilic allylic S_E substitution (see discussions in [10a] [32a,e])

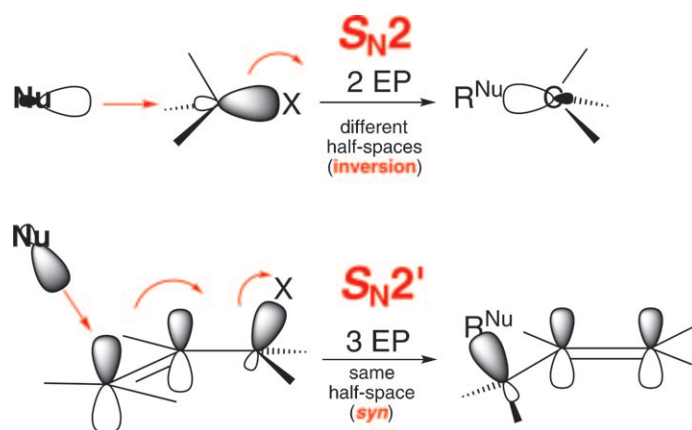


Chart 2. Direct and allylic nucleophilic substitution. For lucid discussions of the S_N2' process with references to the original literature (by G. Stork), see [29a], for the influence of metal ions, see a recent theoretical treatment with extensive citations by Streitwieser *et al.* [29c].

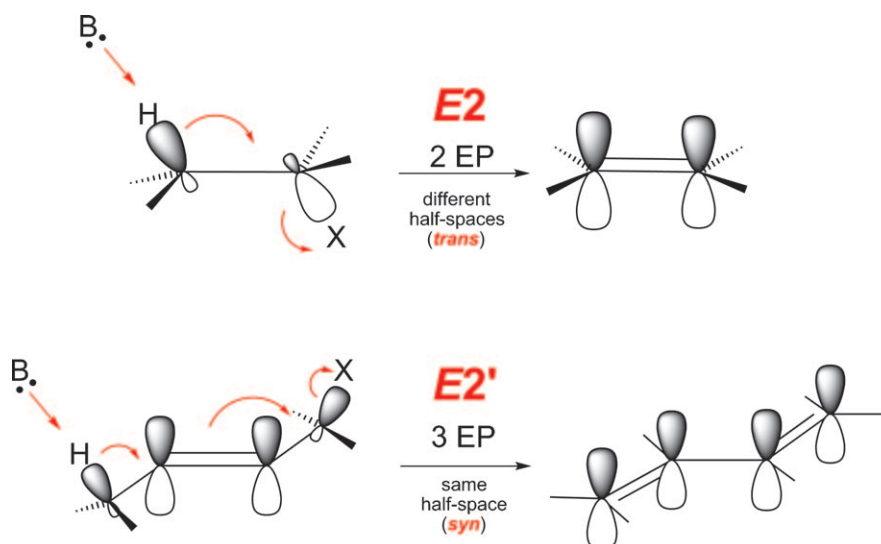


Chart 3. 1,2- and 1,4-Elimination. The formation of a C=N bond from an amino compound with an α -leaving group may be considered an extreme version of an E2-type elimination (*cf.* Scheme 4, center, Fig. 9,a, and [34])

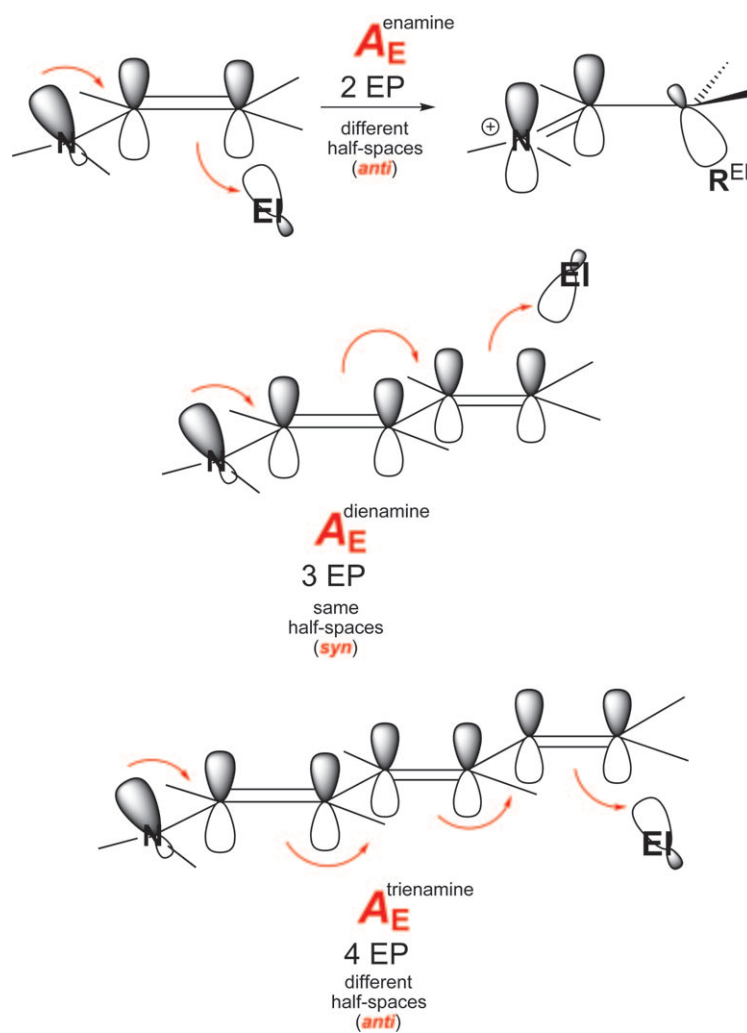


Chart 4. Comparison of the expected steric courses of electrophilic additions to an enamine (cf. Chart 1), a dienamine, and a trienamine in 2-, 4-, and 6-position, respectively. An example corresponding to the trienamine case has actually been described by Breslow and co-workers [29b].

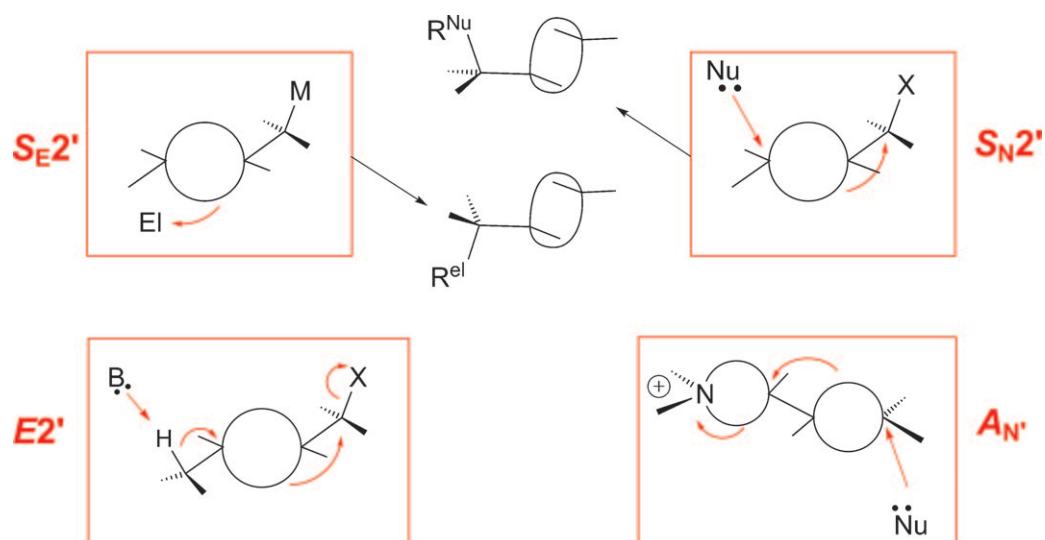


Chart 5. Use of the bent-bond or τ -model for describing the stereochemical course of allylic substitutions (cf. Charts 1 and 2), of a 1,4-elimination (cf. Chart 3), and of conjugate addition to an α,β -unsaturated iminium ion (cf. Fig. 9). For a review article, see [32b].

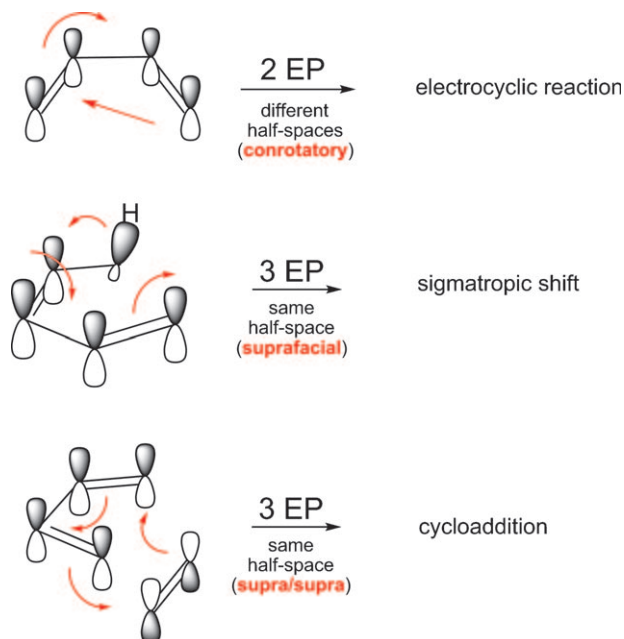


Chart 6. Application of the 'half-space rule' [31] to some pericyclic reactions [27][28]. For an early review article in German, see [27b].